

1 Ion mobility spectrometry-mass spectrometry (IMS-MS) of small 2 molecules: separating and assigning structures to ions

3
4 **Cris Laphorn, Frank Pullen* and Babur Z. Chowdhry**

5 University of Greenwich, School of Science, Medway Campus, Chatham, Kent ME4 4TB, UK

6 Frank.Pullen@greenwich.ac.uk
7

ACCEPTED FOR PUBLICATION

This is the peer reviewed version of the following article: C. Laphorn, F. Pullen, and B. Z. Chowdhry, "Ion mobility spectrometry-mass spectrometry (IMS-MS) of small molecules: Separating and assigning structures to ions," *Mass Spectrometry Reviews*, vol. 32, no. 1, pp. 43–71, 2013 which has been published in final form at <http://dx.doi.org/10.1002/mas.21349>

This article may be used for non-commercial purposes in accordance With Wiley Terms and Conditions for self-archiving. <http://olabout.wiley.com/WileyCDA/Section/id-817011.html>

8 9 10 (ABSTRACT)

11 *The phenomenon of ion mobility (IM), the movement/transport of charged particles under the*
12 *influence of an electric field, was first observed in the early twentieth Century and harnessed later in*
13 *ion mobility spectrometry (IMS). There have been rapid advances in instrumental design,*
14 *experimental methods and theory together with contributions from computational chemistry and gas-*
15 *phase ion chemistry which have diversified the range of potential applications of contemporary IMS*
16 *techniques. Whilst IMS-mass spectrometry (IMS-MS) has recently been recognized for having*
17 *significant research/applied industrial potential and encompasses multi-/cross-disciplinary areas of*
18 *science, the applications and impact from decades of research are only now beginning to be utilised*
19 *for 'small molecule' species. This review focuses on the application of IMS-MS to 'small molecule'*
20 *species typically used in drug discovery (from 100 to 500 Da) including an assessment of the*
21 *limitations and possibilities of the technique. Potential future developments in instrumental design,*
22 *experimental methods and applications are addressed.*

23
24 *The typical application of IMS-MS in relation to small molecules has been to separate species in fairly*
25 *uniform molecular classes such as mixture analysis, including metabolites. Separation of similar*
26 *species has historically been challenging using IMS as the resolving power, R , has been low (from 3-*
27 *100) and the differences in collision cross-sections that could be measured have been relatively small,*
28 *so instrument and method development has often focused on increasing resolving power. However,*
29 *IMS-MS has a range of other potential applications that are examined in this review where it displays*
30 *unique advantages, including: determination of small molecule structure from drift time, 'small*
31 *molecule' separation in achiral and chiral mixtures, improvement in selectivity, identification of*
32 *carbohydrate isomers, metabonomics, and for understanding the size and shape of small molecules.*
33 *This review provides a broad but selective overview of current literature, concentrating on IMS-MS,*
34 *not solely IMS, and small molecule applications.*

35
36 **Keywords:** ion-mobility mass spectrometry; ion mobility spectrometry; mass spectrometry; small
37 molecule; mass-mobility correlation; collision cross-section; ion mobility; FAIMS; drift-time; travelling
38 wave; structural; computational; differential mobility spectrometry; differential mobility analyzer
39

40 I. INTRODUCTION TO IMS

41 The existence of ions in the gas-phase was first discovered when investigating changes in the
42 electrical conductance of air (Thomson, 1903) which had previously been thought to be an electrical
43 insulator. Further work established the generation of ions by UV and X-ray from work by Thomson and
44 Rutherford (1896), Roentgen (1896) and Rutherford (1897)). The rudimentary scientific tools available
45 at the time did not allow a comprehensive understanding of ion behaviour but the behaviour of simple
46 gas-phase ions in a weak electric field was further elucidated by Langevin (1905), who demonstrated

47 that air was a mixture of gases and developed models that described these simpler systems
48 remarkably well.

49
50 Thomson and Aston later developed the first mass spectrometer (Aston, 1919) and further research
51 focussed on low pressure studies of ion-molecule systems that, although not directly involving typical
52 ion mobility pressure regimes, accrued knowledge in the behaviour of ion motion in a partial vacuum.

53
54 The rapid uptake of IMS in military and forensic applications (Zolotov, 2006) benefited from the
55 relatively high proton affinity of the analytes (chemical warfare agents, explosives and illicit drugs),
56 low detection limits and miniaturisation of IMS instrumentation. IMS instrumentation was re-designed
57 for the field, used internal calibrant standards and simplified user interfaces allowed their use by non-
58 scientist military and security personnel. IMS instrumentation is now ubiquitous in handheld forensics,
59 cleaning validation and military applications (from border control to explosive testing in war zones).

60
61 Separation in IMS occurs rapidly, in milliseconds, rather than seconds as in chromatography, so IMS
62 is now beginning to be recognised as a powerful separation step which can be utilised post-ionisation
63 using a range of equipment, benefits from robust day-to-day operation and allows size and shape
64 separation and measurement of analytes that cannot easily be derived using other techniques.
65 Miniaturisation, demonstrated so far primarily in overtone IMS and microfabricated Field Asymmetric
66 IMS (FAIMS), is a highly attractive feature and IMS typically has a low detection limit of nanograms
67 and does not require expensive and environmentally damaging solvents.

68 **II. INTRODUCTION TO IMS-MS**

69 The most important aspect of the combination of an IMS separation (typically occurring in the
70 millisecond time-frame) and MS detection (typically occurring in the microsecond time-frame) is that it
71 allows an additional separation step to be obtained on a MS time-frame (e.g. in addition to liquid
72 chromatography), without compromising the speed of MS detection.

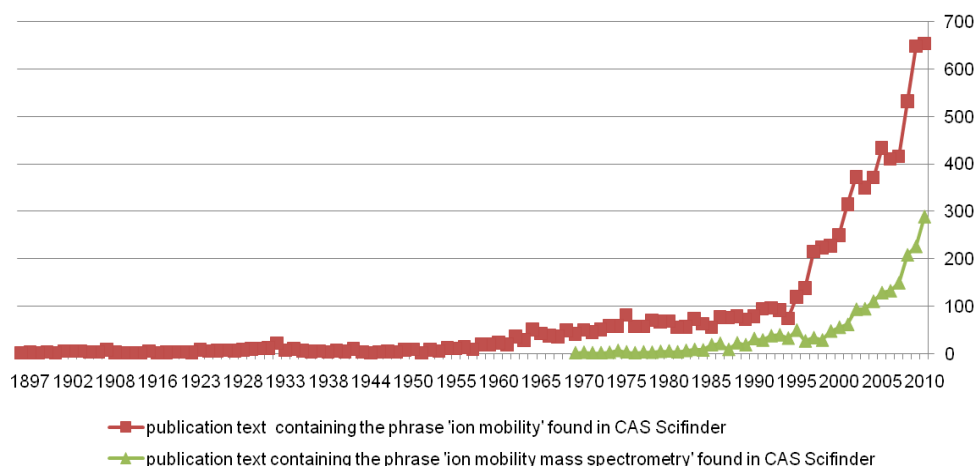
73
74 The work of McDaniel and Martin (1960), Kebarle (1965) and Hogg (1965), Albritton et al., (1968) and
75 later Crompton and Milloy (1977) developed the recognizable configuration of linear drift-tube IMS
76 (DT-IMS). The combination of ion mobility and mass spectrometry allowed more complex studies to
77 be conducted in order to develop models of ion mobility.

78
79 IMS was first hyphenated to a mass spectrometer by Barnes, McDaniel and Martin (1961) using a
80 magnetic sector mass spectrometer; subsequently McAfee and Edelson (1963) described
81 hyphenation to a time-of-flight (TOF) MS. The coupling of IMS with a TOF mass spectrometer is
82 particularly appropriate because the TOF mass spectrometer has the fastest data acquisition rate of
83 any mass spectrometer and can acquire many spectra on the microsecond scale whilst the IMS
84 analytes arrive on a millisecond timescale.

85
86 A review by Hill et al. (2007) describes the early development of IMS-MS with significant contributions
87 and discoveries including those from Bowers, Kemper, Clemmer and Kebarle. IMS has since been
88 interfaced to quadrupole mass spectrometers (Karasek et al., 1976; Wu et al., 1998), quadrupole ion
89 traps (Creaser et al., 2000), linear ion traps and Fourier-transform ion cyclotron mass spectrometers
90 (Bluhm et al., 2000) which is beneficial in terms of a wider linear dynamic range and increased mass
91 spectral resolution. Clemmer et al., (1997) and Creaser et al., (2000) also reversed the stages to
92 produce a MS-IMS design that traps and stores ions in an initial quadrupole ion trap for subsequent
93 ion mobility measurements which has the advantage of pre-concentrating low abundant components.

94
95 Recently IMS has been hyphenated to mass spectrometry systems and the availability of
96 commercially supported instrumentation has arguably led to a rapid increase in the number of
97 publications on IMS-MS, as shown in FIGURE 1. FAIMS, a type of differential mobility spectrometry,
98 originated in Russia in the early 1980s (Gorshkov, 1982) emerged as an analytical tool (Buryakov et
99 al., 1993), and was later commercialised by Ionalytics (Selectra, 2003), as a front-end accessory for
100 MDS Sciex (Concord, Ontario, Canada) mass spectrometer systems (2004), Thermo FAIMS, (2007)
101 and Owlstone Nanotechnologies FAIMS. Waters Inc. (Milford, MA) launched the first generation Synapt
102 Triwave travelling wave IMS system in 2006 and updated with a second generation instrument with
103 improved resolution (G2, 2009) and improvements to sensitivity (G2S, 2011). AB Sciex launched the

104 SelexION ion mobility device in 2011 for their triple quadrupole mass spectrometer and quadrupole-
105 trap mass spectrometer.
106



107
108 **FIGURE 1.** Chart showing number of publications containing the phrases “ion mobility” and “ion
109 mobility mass spectrometry” obtained using CAS Scifinder.

110
111 There has been limited recognition of the potential of IMS-MS analysis for ‘rule-of-5’ type small-
112 molecules (Lipinski et al., 1997) outside of traditional IMS analyte classes (e.g. explosives, chemical
113 warfare and illicit drugs). The historical lack of interest and sporadic periods of development in IMS-
114 MS for small molecule applications seems most likely to be due to perceived poor resolution,
115 strengths in competing chromatographic techniques and weaknesses in the robustness of IMS
116 regarding a poor linear range (Turner and Brokenshire, 1994), “memory effects” from contamination
117 (Gehrke, 2001) and interference from matrices.

118
119 In contrast IMS-MS has been applied to biomolecules including peptides (Harvey, Macphee & Barran ,
120 2011), proteins (60 kDa-150 kDa) and large protein complexes (1- 4 MDa) (Utrecht et al., 2010)
121 particularly after the application of non-covalent mass spectrometry conditions to IMS-MS. Using
122 these especially gentle electrospray ionisation conditions is believed to maintain the weak
123 (cooperative) molecular interactions present in many biomolecular structures and thus avoid
124 fragmentation. Whilst IMS-MS typically lacks the resolution (1% error or 10 nm²) of x-ray or NMR for
125 large molecular weight biomolecules it enables analysis using smaller amount of material, allows
126 analysis of structures >100 kDa that are difficult to analyse by NMR and is, arguably, as realistic an
127 environment as x-ray structures due to lattice effects present. IMS-MS has, therefore, been utilised as
128 a tool to probe the stabilisation of proteins in the presence of ligands and metals (as a unique method
129 of metal speciation; Souza Pessôa et al., 2011), protein-protein-interactions, protein mutants and their
130 structural consequences as well as protein unfolding via various means of ion activation (Jurneczko
131 and Barran, 2011). In addition to detailed understanding of individual biomolecular systems, IMS-MS
132 has also been applied to more high-throughput analytical approaches including screening of
133 phosphorylated peptides (Thalassinos et al., 2009), identification and separation of chemically cross-
134 linked peptides (Santos et al., 2010) and combining topology in protein substructures with proteomics
135 data (Zhou and Robinson, 2010). This review does not attempt to summarise biomolecule analysis by
136 IMS-MS, which is covered by many authors, but rather to contrast the adoption of IMS-MS in
137 biomolecule analysis and focuses on small molecule applications.

138 III. DIFFERENCES IN PERFORMANCE OF IMS-MS AND IMS

139 A. The ion efficiency and resolution challenge

140 Some of the key differences between IMS and hyphenated IMS-MS include the pressure regime in
141 the ion mobility cell, the size of the instrument and the typical ionisation source. Whilst specifications
142 and performance in IMS may be indicative of those in IMS-MS there are some technical reasons why
143 this may not follow. It is critical to note that the results may well be different in IMS-MS compared to
144 IMS especially due to sensitivity issues and pressure regime changes from IMS to MS stages.
145

146 In IMS-MS there are often two main challenges (i) to utilise all the ions from the ionisation source,
 147 (especially in a pulsed IMS separation such as drift-time IMS, but not a challenge in DMS or FAIMS
 148 which typically have a 100% duty cycle if a single transmission voltage is selected) and (ii) elimination
 149 of all neutral species whilst ensuring transmission of ions to the MS stages to maintain sensitivity.
 150 Traditionally DT-IMS-MS sensitivity has been estimated to be inversely proportional to the IMS
 151 resolving power squared; ion losses at the IMS exit aperture ranging from 99 to 99.9% (Tang et al.,
 152 2005) and ion introduction losses being between 99.6 to 99.9% (Belov et al., 2008). The desire to
 153 increase the gas pressure in the DT-IMS cell to increase resolution must therefore be balanced with
 154 the possibility that it may well reduce ion transmission by requiring a reduction of the aperture size in
 155 the interface from IMS to MS. The different pressure regimes in IMS systems are described in Table 1.
 156

157 For DT-IMS-MS the drift gas pressure must be increased proportionally to electric field strength in
 158 order to maintain a low E/N ratio ($< 2 \times 10^{-17} \text{ Vcm}^2$), required to obtain field-independent mobilities for
 159 which the simplified Mason-Schamp equation (Mason and McDaniel, 1988) holds:
 160

$$161 \quad K = (3q/16N)(2\pi / \mu kT)^{1/2} 1/\Omega \quad (1)$$

162
 163
 164
 165 Where K is the ion mobility, q is the ionic charge, N is the buffer gas density, μ is the reduced mass
 166 of the buffer gas and the ion, k is the Boltzman constant, T is the temperature and Ω is the collision
 167 cross-section (CCS).
 168

169 For Travelling Wave Ion Mobility-MS (TWIMS-MS) the gas pressure must also be increased
 170 proportionally to the electric field, such that:
 171

$$172 \quad K = K_o N_o / N = KP_o T / (PT_o) \quad (2)$$

173
 174
 175 where K is the ion mobility, N is the buffer gas density, N_o is the Loschmidt number (the value of N
 176 at standard temperature ($T_o = 273\text{K}$) and pressure ($P = 1 \text{ Atm}$) and K_o is the reduced ion mobility.
 177

178
 179 **TABLE 1.** Pressure regimes in typical IMS systems.
 180

Type of IMS system	Pressure regime	Typical operating pressure
Ambient DT-IMS	Ambient pressure	1000 mbar (Kanu et al., 2008)
Reduced pressure DT-IMS	Reduced pressure	10^{-5} (Ruotolo et al., 2002b) to 1.3 (Valentine et al., 2001) mbar
FAIMS or DMS	Ambient pressure- >ambient pressure	400 to 1571 mbar (Kolakowski and Mester, 2007)
Travelling wave IMS	Reduced pressure	0.5 mbar (Waters Synapt G1) to >3 mbar (Waters Synapt G2) (Giles et al., 2011)
Differential mobility analysis	Ambient pressure	1013 mbar

181
 182 Approaches to maximise sensitivity include utilising quadrupole and octopole ion traps (Henderson et
 183 al., 1999; Creaser et al., 2000; Myung et al., 2003) and electrodynamic ion funnels (Wytenbach et al.,
 184 2001) to accumulate and introduce ions efficiently from the ion source to increase the sensitivity of
 185 DT-IMS. Multiplexing approaches including Hadamard (Clowers et al., 2006) and Fourier-type (Tarver,
 186 2004) gating techniques have also been utilised for increasing the sensitivity of DTIMS, by increasing
 187 the frequency of ion injection events and thus increasing the quantity of ions injected into DT-IMS by
 188 up to 50%. Most of these approaches have been integrated into full IMS-MS systems with dramatic
 189 improvements in sensitivity.
 190

191 There is some uncertainty in the identification of the ions in their transmission through the IM cell and
 192 it seems clear that hyphenating IMS and MS allows a more comprehensive understanding of the

193 ionisation processes and fragmentation pathways in IMS. For example, when using a radioactive ^{63}Ni
 194 cell, proton transfer to the analytes should lead to protonated monomer and dimer ions; however,
 195 without a mass spectrometer as the detector, the identification of the ions in the ion cell cannot be
 196 unambiguously ascertained. Indeed, a comparison of limonene and 2-nonanone by IMS and IMS-MS
 197 resulted in a variety of unexpected fragments and ions, resulting in a non-trivial IMS spectrum and
 198 making interpretation of the results difficult (Vautz et al., 2010). Any unambiguous identification of ions
 199 in IMS will be important both in structural measurements (size, shape and topology) and for
 200 comparison of related IMS techniques (e.g. TWIMS-MS) that often use historical DT-IMS-MS data as a
 201 calibration standards in ion mobility and collision cross-section calculations.

202 **B. Features of IMS techniques utilised in IMS-MS**

203 IMS-MS potentially provides a number of advantages over and above IMS including:

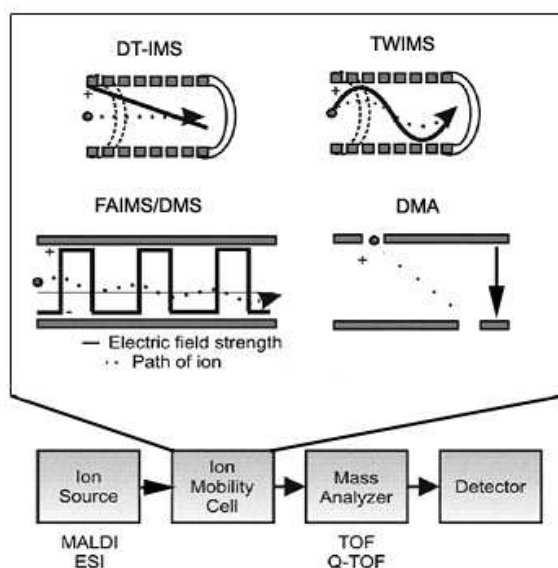
- 204 i) as a rapid gas-phase separation step before mass spectrometry analysis,
- 205 ii) the identification of ions subsequent to characteristic drift times by comparison with data
 206 acquired under comparable conditions,
- 207 iii) measurements of collision cross-sections and derivation of further information about size and
 208 shape, either by comparison with computational modeling or by analysis within a series of
 209 compounds
- 210 iv) better characterisation of ion and ion-neutral ion mobilities by simultaneous acquisition of
 211 mass spectrometry data, and
- 212 v) better characterisation of ionisation (Tang et al., 2006) and fragmentation pathways via a
 213 better understanding of gas-phase ion structures

214
 215 IMS has been hyphenated to liquid chromatography, gas chromatography (Baim and Hill, 1982;
 216 Snyder et al., 1993), super-critical fluid chromatography (Eatherton et al., 1986; Huang et al., 1991),
 217 ions produced via matrix assisted laser desorption ionisation (Jackson et al., 2007), desorption
 218 electrospray ionisation (Weston et al., 2005), pulsed corona discharge ionisation (Hill and Thomas,
 219 2003) and miniaturised to microchip scale (Shvartsburg et al., 2009b).

220
 221 IMS-MS systems are typically composed of four stages (Figure 2):

- 222 1) an ion source e.g. MALDI or electrospray that generates ions. Electrospray ion sources have
 223 been preferred for retaining native-like structures in biological systems.
- 224 2) an IMS cell, where charged particles migrate under the influence of an electric field.
- 225 3) a mass analyzer, typically a time-of-flight (TOF) mass spectrometer which is designed to
 226 allow a fast acquisition rate and large mass detection range.
- 227 4) an ion detector.

228



229

230 **FIGURE 2.** Overview of typical ion-mobility mass spectrometer configurations, adapted from Enders
 231 and Mclean, 2009.

232 There are four main types of IM cell utilised in IMS-MS.

233 (i) Drift-time IMS (DT-IMS) is the simplest configuration where collision cross-section (CCS) can
234 be directly calculated without calibration and provides the highest resolving power. A tube is
235 filled with a buffer gas (or mixture) and a low voltage field is applied, typically from 5 to 100
236 Vcm^{-1} . The ions collide with neutral buffer gas molecules, exit via a detector and the collision
237 cross-section Ω_T , at a temperature T can be obtained by measuring the velocity of the ions
238 and solving the Mason-Schamp equations at intermediate electrical fields (5-100 Vcm^{-1}):
240

$$V_d = KE \quad (3)$$

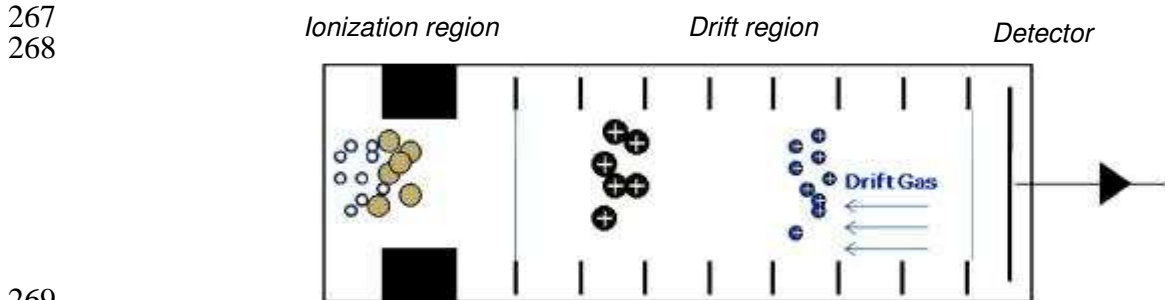
241 where v_d is the drift velocity of the ion, K is the ion mobility, E is the imposed electric field,
242 and
243

$$\Omega_T = \left(\frac{3ze}{16N} \right) \left(\frac{2\pi}{\mu kT} \right)^{1/2} \left(\frac{1}{K} \right) \quad (4)$$

246 where z is the numerical charge, e is the elementary charge, N is the number density of the
247 buffer gas, μ is the reduced mass of the ion- buffer gas neutral pair, k is the Boltzmann
248 constant and T the temperature in Kelvin.
249

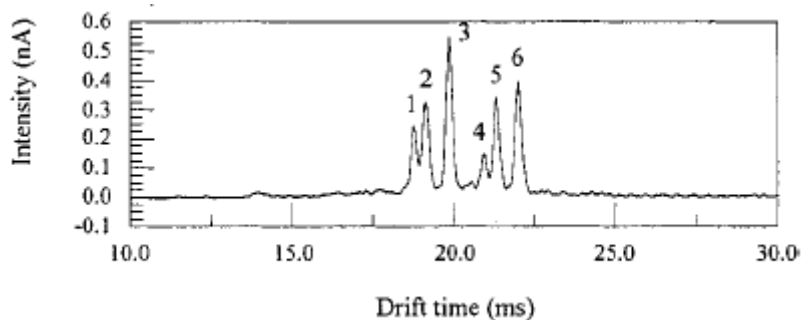
251 DT-IMS suffers from an inherent lack of sensitivity, due to a pulsed analysis (where ions are
252 measured in packets), and the subsequent loss in duty cycle, as the time between packets of
253 ions is not utilised. A review of IMS by Eiceman and Karpas (2004) discusses the history of
254 IMS, the chemistry and physics of ion behaviour and reflects on the potential future
255 development and applications of IMS.
256

257 In linear DT-IMS, illustrated in FIGURE 3, the sample is introduced to an ionisation region
258 where ionisation can take place by a number of methods including β -emission from a ^{63}Ni
259 corona discharge, photo-ionisation, electrospray etc. Ions are allowed through an electric
260 shutter grid, whilst neutrals remain in the ionisation source and the measurement time is
261 initiated. The drift tube can vary in length from 5 centimetres to 3 metres or more. An electric
262 field gradient, typically from 10-100 Vcm^{-1} , from the ionisation source to the detector causes
263 the ions to traverse the drift tube at a constant velocity. A drift gas is introduced counter-
264 current to the flow of ions keeping the drift-tube free of neutrals which could participate in ion-
265 neutral clusters.
266



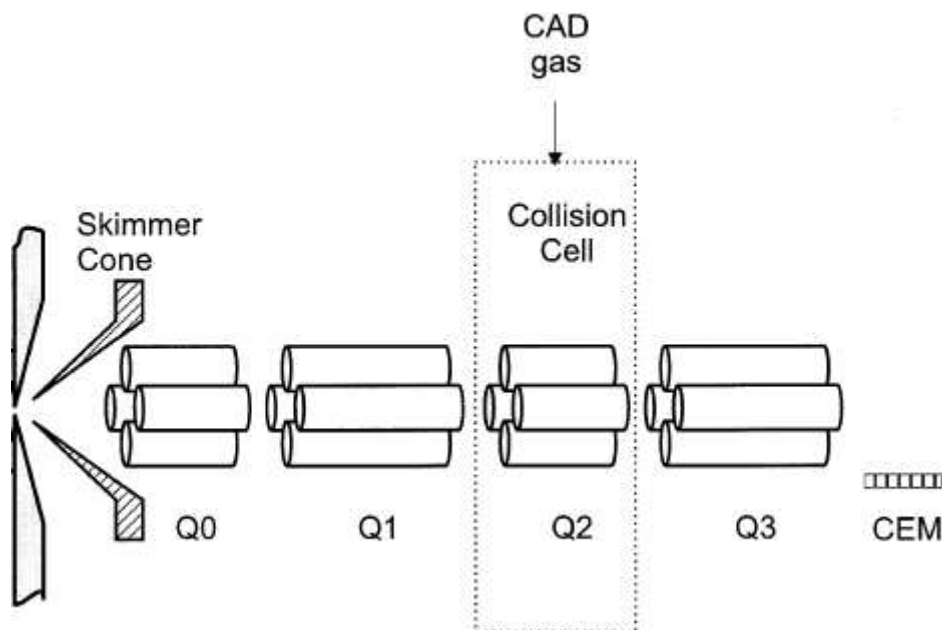
269
270 **FIGURE 3.** Illustration of DT-IMS, adapted from Eiceman and Karpas (2004). A voltage
271 gradient is applied to the ions from left to right.

272 The total ion signal is detected and plotted with respect to time to form an ion mobility
273 spectrum, e.g. (see FIGURE 4) for a mixture of amphetamines analysed by ESI-DT-IMS-MS
274 (Matz and Hill, 2002). Smaller ions travel faster through the drift region and have shorter drift
275 times, compared to higher molecular weight ions that drift slower and possess longer drift
276 times.
277
278



279
 280 **FIGURE 4.** ESI-DT-IMS-MS spectrum of a mixture of 1) amphetamine, 2) methamphetamine,
 281 3) ethylamphetamine, 4) 3,4-methyldioxyamphetamine, 5) 3,4-methylenedioxy methamphetamine and
 282 6) 3,4-methylenedioxyethylamphetamine, adapted from Matz and Hill (2002a).

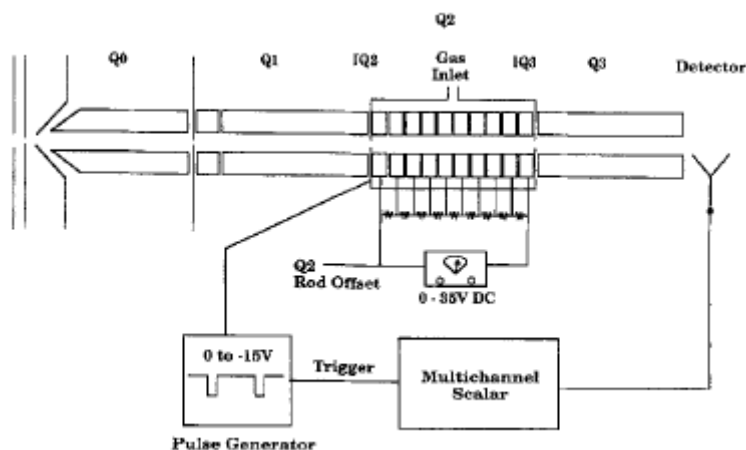
283 Another complementary approach to classical DT-IMS-MS was the use of the second quadrupole
 284 (Figure 5) in a triple-quadrupole mass spectrometer as an ion mobility device; while this approach
 285 was never commercialized it did open up opportunities in hyphenation of IMS and MS. In the triple
 286 quadrupole energy loss method an incident ion is transmitted to the second quadrupole of a triple
 287 quadrupole mass spectrometer where the ion will experience a drag coefficient and generate a
 288 stopping curve; from the stopping curve the ion mobility can be measured and a collision
 289 cross-section determined. Indeed, Covey and Douglas (1993) were the first to measure collision
 290 cross-sections for some biomolecules using this method and also later reviewed collision dynamics in
 291 quadrupole systems including an assessment of the internal energy of the $C_6H_5^+$ ion by measuring the
 292 increase in collision cross-section after collisional activation (Douglas, 1998).



293
 294 **FIGURE 5.** Schematic of the triple quadrupole configuration that can be used to obtain ion mobility
 295 measurements via an energy loss method, adapted from Purves et al. (2000).

296 This triple-quadrupole energy loss method was further developed to utilise segmented collision cell
 297 rods separated by small 1 mm gaps that enabled a radio-frequency only quadrupole drift cell to be
 298 used to reduce ion losses due to diffusion and enable mass selection before or after the drift cell, and
 299 a DC gradient that moved the ions in an axial direction (see Figure 6, Javahery & Thomson, 1997).
 300 Unfortunately this configuration was outside the typical low-field IMS range and may have resulted in
 301 field-heating of ions. This configuration was later improved to possess an increased gas pressure and
 302 lower field concentration that resulted in minimal internal excitation of the ions (Guo et al. 2004).

303
 304
 305



306
307
308
309

310 **FIGURE 6.** Schematic of a segmented triple quadrupole configuration that can be used to obtain ion
311 mobility measurements, adapted from Javahery & Thomson (1997).

312

- 313 (ii) Differential mobility IMS (DMS) or FAIMS uses a sequence of intermediate and high field
314 regimes where the behaviour of ions is described empirically by the Mason-Schamp equation
315 (Mason and McDaniel, 1988) under a high-field regime, which can be expanded to an infinite
316 series of E/N :

317

$$318 K_0(E) = K_0(1 + a(E/N)^2 + b(E/N)^4 + c(E/N)^6 + \dots) \quad (5)$$

319

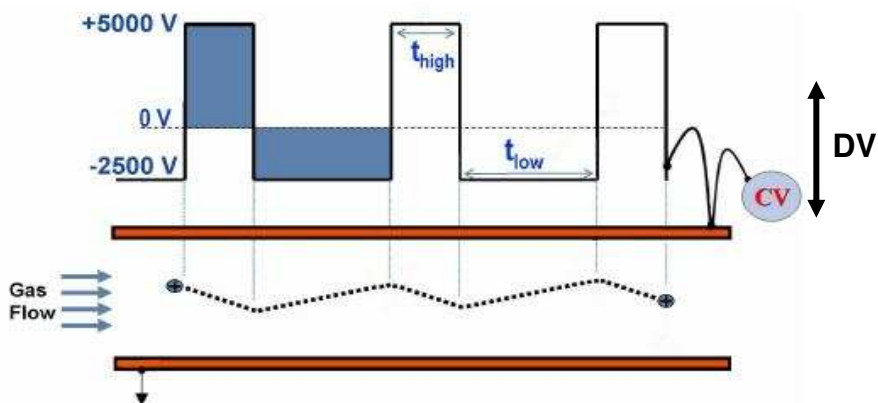
320

321

322 where K_0 is the reduced ion mobility, E is the field intensity and N is the buffer gas number
323 density. However, under a typical FAIMS electric field the mobility can be approximated by
324 using the first two factors as the importance of the sixth order and higher are insignificant (the
325 fourth order is two orders of magnitude smaller than second order, and the second order is
326 three to five orders of magnitude smaller than one (see Shvartsburg et al., 2004).

327

328 The basic principle of operation is that ions are introduced to a region with electrodes and a
329 stream of gas acts as a transport medium. An asymmetric waveform is passed across the
330 electrodes, which consists of a high potential electric field for a short time followed by a low
331 potential electric field for a longer time; this typically fixed dispersion voltage (DV) waveform is
332 superimposed with a variable compensation voltage (CV) to maintain a stable trajectory for
333 the analyte ion. This process will effectively select ions and act as an ion filter, as shown in
334 Figure 7. A cylindrical electrode configuration has usually been designated FAIMS, whereas
335 parallel plate configurations have typically been designated as DMS.

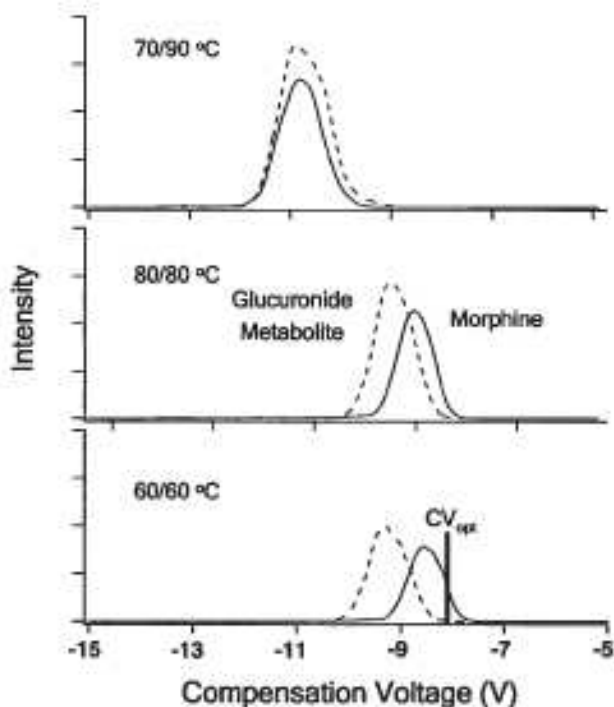


336

337 **FIGURE 7.** Illustration of an example of a parallel plate DMS with compensation voltage applied
 338 showing ion transmission, adapted from Thermo Fisher Scientific Inc., FAIMS Operators manual
 339 (2007).

340

341 A compensation voltage scan measurement (Figure 8) shows a typical profile attained by
 342 optimising the effect of inner and outer electrode temperatures on peak profile for morphine
 343 and its 3-β-D-glucuronide metabolite (Hatsis et al., 2007). Optimising the separation of
 344 morphine whilst maintaining sensitivity was reported to enable the metabolite interference to
 345 be effectively filtered out, and significantly improve the quantification of morphine.



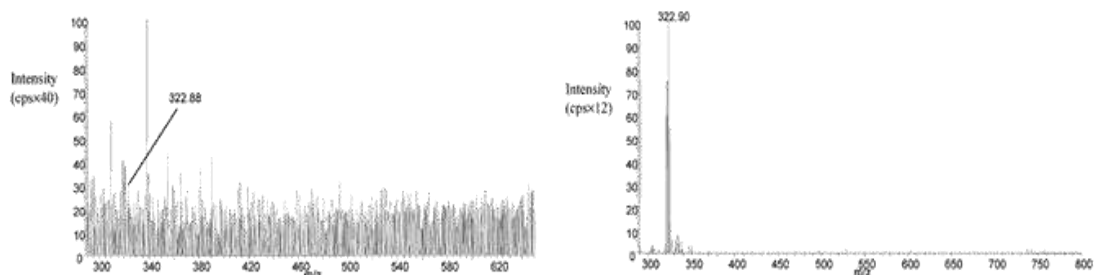
346

347 **FIGURE 8.** Compensation voltage scans of morphine and the glucuronide metabolite, adapted from
 348 Hatsis et al., (2007).

349

350 The use of compensation voltage optimisation to select an analyte ion can result in a clear difference
 351 in the mass spectrum observed resulting in an increased S:N ratio for the analyte and a reduction in
 352 other signals as shown in the use of ESI-FAIMS-MS with cisplatin and its hydrolysis products (Cui et
 353 al., 2003) shown in FIGURE 9.

354



355
 356 **FIGURE 9.** Mass spectra showing the reduction in background noise from (a) ESI-MS to (b) ESI-
 357 FAIMS-MS, adapted from Cui et al. (2003).

358 Currently the factors determining the separation mechanism in FAIMS or DMS and factors
 359 governing peak width as well as transmission remain relatively difficult to predict (Shvartsburg
 360 et al., 2004). The parameters influencing performance include field intensity, ion path length,
 361 gas properties (composition, temperature, pressure), shape and width of electrodes, the
 362 profile and frequency of asymmetric waveform, compensation voltage scan speed and gas
 363 flow. Champarnaud et al., (2009) studied the separation of trace level impurities by combining
 364 experimental observation with a Design of Experiment (DOE) statistical treatment that
 365 indicated important factors in the optimisation of the values of the compensation voltage,
 366 signal intensity, separation, peak asymmetry and peak width. However, a study of
 367 tetraalkylammonium ions found standard conditions were often suitable for selecting ions with
 368 an m/z value of 100-700 (Aksenov and Kapron, 2010). The simulation of ion motion in planar
 369 electrode FAIMS and cylindrical electrode FAIMS, provided insights into design, experimental
 370 variables and interpretation (Smith et al., 2009b) and some of the key molecular and
 371 instrumental parameters affecting performance were discussed by Nazarov (2006) and Levin
 372 et al. (2004).

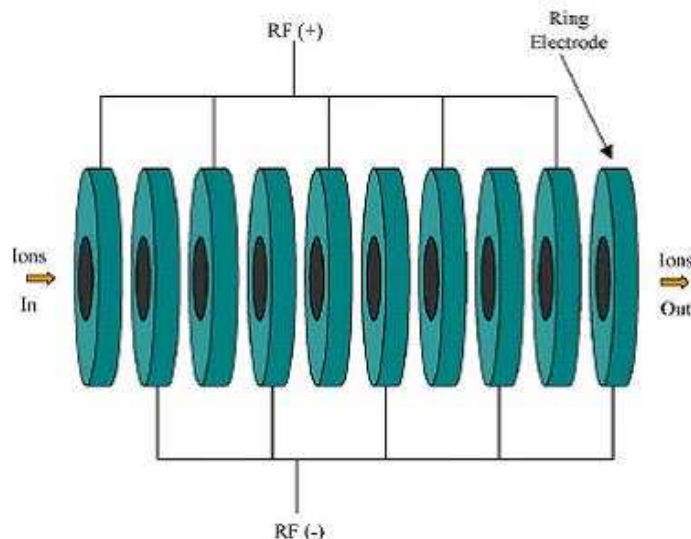
373
 374 Whilst there are several novel geometries (Prieto, 2011), there are two main forms of field
 375 asymmetrical waveform ion mobility spectrometers: 1) those with planar electrode geometry
 376 and 2) those with curved electrode geometry. Both planar geometry and the curved
 377 geometries of FAIMS and DMS evolved during the 1990s, and in the early 1990s the term
 378 differential mobility spectrometry (DMS) became generally synonymous with planar
 379 electrodes and the term FAIMS became synonymous with curved geometries, although there
 380 are multiple examples of overlapping usage of the terms DMS and FAIMS. One of the primary
 381 differences relates to the use of polar transport gas modifiers. Planar devices create
 382 homogeneous electric fields which enables the use of transport gas modifiers without
 383 resolution losses whereas curved geometries tend to create inhomogeneous fields which lead
 384 to a loss in resolution when using transport gas modifiers. However, curved geometries have
 385 been shown to provide some degree of ion focusing at atmospheric pressure resulting in
 386 higher sensitivity (Guevremont & Purves, 1999; Krylov, 1999). Planar line-of-sight analyzers
 387 enjoy the convenience of transmitting all ions when the RF voltages are turned off, so that
 388 operation without mobility separation can be achieved simply by turning off the fields. Curved
 389 geometry/non line-of-sight FAIMS require the device to be removed for operation without
 390 mobility separation. A wider analysis of the differences between alternative geometries was
 391 described by Krylov (2003).

392
 393 A comprehensive review discussed the applications of FAIMS for drinking water analysis,
 394 pharmaceutical metabolite identification and separation of isomers and isobaric peaks
 395 (Kolakowski and Mester, 2007). In addition a detailed account of the fundamentals of DMS
 396 and FAIMS has been written by Shvartsburg (Shvartsburg, 2010).

- 398 (iii) Travelling wave ion mobility spectrometry (TWIMS) is a novel method whereby ions are
 399 separated according to their mobility in a series of voltage pulses in a travelling wave (T-wave)
 400 mobility cell utilising RF ion guides (Gerlich, 1993). The resolving power is relatively low;
 401 however, collision cross-sections can be derived by calibration with known standards. This ion
 402 mobility approach has been successfully interfaced to a conventional time of flight mass
 403 spectrometer and, due to the trapping gates and fast data acquisition rate of the TOF, good
 404 sensitivity is achieved. Despite attempts (Shvartsburg and Smith, 2008; Smith et al., 2009a)

405 the motion of ions in TWIMS is not fully understood and TWIMS calibration is typically used to
406 calculate CCS values. The commercial technical and software support has arguably
407 reinforced attempts to utilise IMS-MS in separation, characterization and measurement
408 applications, for example, via the routine use of multidimensional data in Driftscope software
409 (Williams et al., 2009a) and software to process complex data such as time-aligned parallel
410 fragmentation (D'Agostino and Chenier, 2010).
411

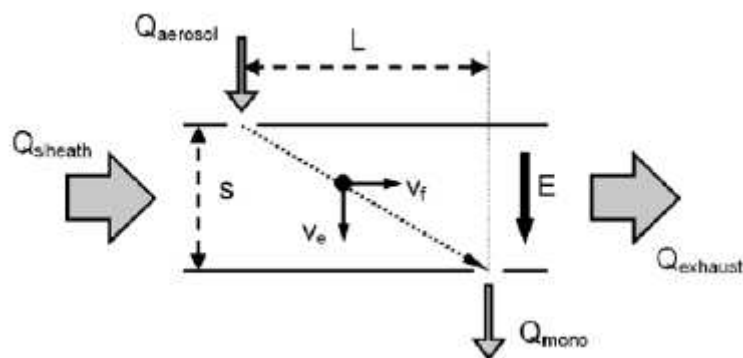
412 In travelling wave ion mobility spectrometry a transient DC voltage pulse is applied in order to
413 create an electromotive force via a series of sequentially opposite polarity RF-only rings
414 to create a travelling wave which propels ions through the device, as shown in Figure 10. Ions
415 with high ion mobility slip behind the wave less often (or spend more time surfing) than ions of
416 low ion mobility thus enabling separation based on relative ion mobility.



417
418 **FIGURE 10.** Illustration of a stacked ring ion guide used in traveling wave ion mobility spectrometry
419 (TWIMS), adapted from Pringle et al. (2007).

420 Visualising data obtained using the proprietary Driftscope software enables a range of options
421 for understanding the data including 3D visualisation, 2D plots and intensity views etc, The
422 data can be interactively processed if desired, for example, to show data that only contains a
423 certain component using various geometric selection tools such as lasso and square area.
424
425

426
427 (iv) The Differential Mobility Analyser (DMA) was originally developed to generate particles in
428 order to calibrate aerosol instruments, later expanded to describe the mobility of non-diffusing
429 particles by Knutson and Whitby (1975) and recently to describe the mobility of diffusing
430 particles by Stolzenberg & McMurray (2008). The DMA consists of a combination of electric
431 field mobility in addition to a fast gas stream, only ions with a well defined electrical mobility
432 are transmitted into an outlet slit leading to the mass spectrometer inlet (see Figure 11). The
433 DMA vacuum regime means that the measured ions do not experience a vacuum interface or
434 ion guide so may be less prone to structural modifications (Hogan et al., 2011) and, as the
435 separation technique is a space-dispersion rather than a time-dispersion technique, the ions
436 can be continuously transmitted to a mass spectrometer.
437
438
439



440

441 **FIGURE 11.** Schematic of the operation of a differential mobility analyzer. Ion are injected at the top
 442 left and move downwards and to the right, over a distance S , under the influence of an electric field E ,
 443 adapted from de la Mora et al., (2006)

444 The DMA technique may be considered a hybrid of DT-IMS and DMS as the separation
 445 process is based on the low electric field mobility like DT-IMS, however the sampling is
 446 continuous as in DMS. DMA-MS has been most widely explored for large molecules; however,
 447 discussion on multiple charged polyethylene glycol ions (Ude et al. 2004) illuminated
 448 structures from approximately 300 Da to 3000 Da describing configurations for long straight
 449 chain molecules. One of the advantages of DMA is that it can, theoretically, be easily added
 450 to existing mass spectrometry stages without complex interfaces due to operation at
 451 atmospheric pressure (Rus et al., 2010). A DMA was coupled to an existing Sciex QStar MS
 452 (Concord, ON, Canada) enabling separation of L-alanine and an isomer, sarcosine,
 453 (Martínez-Lozano P et al., 2010) which are proposed to be small molecule biomarkers from
 454 urine in the progress of prostate cancer.
 455

456 IMS covers a range of different techniques and unfortunately some gross simplifications have resulted
 457 in terminology that may be confusing.

- 458 1. DTIMS is also known as Classical IMS, Conventional IMS, Standard IMS, Drift-Tube IMS, Time of
 459 flight IMS, Traditional IMS, Plasma Chromatography and Ion Chromatography.
- 460 2. DMS includes High Field Asymmetric Waveform IMS (FAIMS), Field Ion Spectrometry and Ion
 461 mobility Spectroscopy and is commercialised in the Ionalytics Selectra, Thermo FAIMS, Owlstone
 462 Nanotechnologies and AB Sciex Selectra systems.
- 463 3. Travelling wave ion mobility spectrometry (TWIMS) is commercialised in the Waters Synapt
 464 systems.
- 465 4. Differential Mobility Analysers (DMA) have been developed by several groups at Yale (USA),
 466 CIEMAT (Madrid) and RAMEM (Madrid).

467 **Comparison of key benefits and challenges of IMS-MS methods**

468 There is currently a wealth of IMS-MS systems available both commercially and being used and
 469 developed in academic institutions.
 470

471 DT-IMS-MS has been most widely used in academic institutions and provided some of the highest
 472 resolving powers. An advantage of DT-IMS-MS is that the ion mobility can be determined
 473 experimentally and collision cross section determined without requiring calibration. A key challenge is
 474 that the pulsed analysis leads to an inherent loss of duty cycle and hence reduction in sensitivity.
 475

476 An advantage of both DMS-MS and FAIMS-MS is that it operates as a continuous device when the
 477 compensation voltage is selected so does not have the 'lossy' sampling issues of DT-IMS and TWIMS.
 478 The separation appears to be orthogonal to m/z and sometimes size so that separations may be
 479 uniquely tuned to select a chosen analyte and thus be used as a powerful separation technique. A
 480 key challenge is that it has proven difficult to definitively assign structural properties and changes to
 481 DMS measurements as several factors appear to contribute to the clustering/declustering mechanism
 482 and analyte drift times thus it appears to be best utilized as a separation device.
 483

484 An advantage of TWIMS-MS is that it is commercially supported and that the ion mobility can be
 485 determined experimentally and collision cross-section determined with suitable calibration. Whilst the
 486

487 resolution obtained in TWIMS is typically lower than dedicated DT-IMS-MS and some FAIMS/DMS
488 the software to interpret and process the complex data is well supported.

489
490 Advantages of DMA-MS include operation in the low electric field regime that typically means less
491 structural distortions and determination of collision cross-section, a continuous sampling rate that
492 should mitigate sensitivity losses (with reported transmission efficiencies of up to 50% (Martínez-
493 Lozano et al., 2011)) and the theoretical ability to add the device as a front-end to many existing mass
494 spectrometer systems. However DMA-MS has not been fully commercialized yet or utilized for the
495 multitude of “small molecule” applications explored in DT-IMS-MS, FAIMS-MS, DMS-MS and TWIMS-
496 MS though it shows significant promise.

497 **C. Understanding IMS-MS resolving power and selectivity**

498 IMS can separate analytes based on their ion mobility including closely related species such as
499 isomers (Williams et al., 2010), isobars and isotopomers (Shvartsburg et al., 2010a). The key
500 parameters affecting a useful separation are 1) the resolving power and 2) the selectivity.

501 **Resolution and peak capacity in IMS**

502 The combination of ion mobility and mass spectrometry in IMS-MS offers a technique that is able to
503 distinguish components based on their size to charge ratio (Ω/z for IMS) and mass to charge ratio
504 (m/z for MS), thereby enabling orthogonal specificity. Even with expensive high-resolution mass
505 spectrometer systems affording $m/\Delta m_{50\%}$ resolution of over 400,000 it is still analytically challenging to
506 differentiate between isomeric components and often complex MSⁿ experiments are required to
507 achieve selectivity for unambiguous assignment. Ion mobility can provide extra resolving power,
508 however IMS used alone is currently unable to unambiguously identify an unknown molecular
509 component without *a priori* knowledge of the measured drift time.

510
511 It is possible to measure the resolving power of ion mobility using a single quotient definition (Siems
512 et al., 1994):
513

$$R = dt / wh \quad (6)$$

514
515 where R is the resolving power of the IMS, dt is the drift time of the ion of interest and wh is the full
516 peak width measured at half height. Resolving power is a measure of the efficiency of an instrument
517 to separate two peaks. The Waters Synapt G2 IMS system has been developed to encompass a
518 resolving power of up to 40; FAIMS resolving powers of up to 100 (Shvartsburg et al., 2010b) have
519 been achieved, and several reports of resolving powers of up to 225 with DT-IMS have been reported
520 (Koeniger et al., 2006; Shelimov et al., 1997; Kemper et al., 2009). Developments including higher
521 pressure trapping and focussing (Clowers et al., 2008), overtone ion-mobility (Valentine et al., 2009)
522 and circular instruments (Bohrer et al., 2008) are expected to exceed these current limitations.

523
524 The number of theoretical plates is a mathematical concept, relevant in any chromatographic
525 technique, which is often used to describe column efficiency and is an indirect measure of the peak
526 width for a peak at a specific retention time:
527

528

$$N = 5.545 \left(\frac{t_R}{W_h} \right)^2 \quad (7)$$

529
530 where N = number of plates, t_R = retention time and W_h = peak width at half height (in units of time).
531 The number of theoretical plates is typically used to compare chromatographic systems and the data
532 in Table 2 compares various types of IMS with typical traditional chromatographic techniques.

537 **TABLE 2.** A comparison of required resolving power in theoretical plates for various types of IMS
538 compared to typical chromatographic conditions.

539

Approximate number of theoretical plates	Required resolving power of equivalent	Comparative chromatography conditions
--	--	---------------------------------------

	IMS	
20000	60	High performance liquid chromatography (HPLC)
80000	120	Ultra high performance liquid chromatography (UHPLC)
125000	150	Gas chromatography (GC)
222000	200	High resolution IMS (Asbury & Hill, 2000a)
887000	400	Capillary electrophoresis (CE)

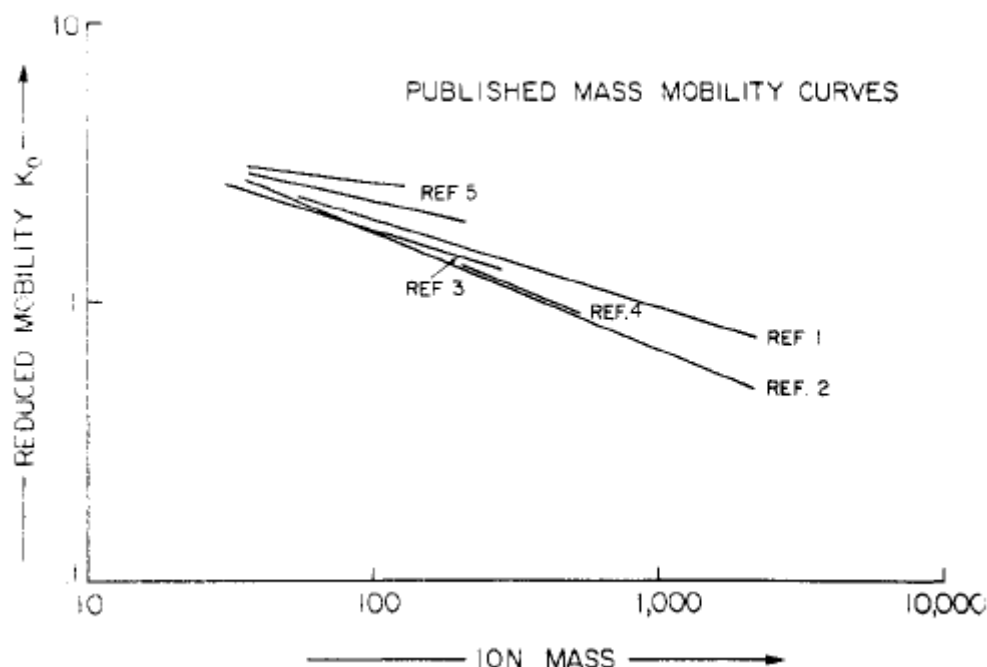
540
541
542
543
544
545
546
547
548
549
550
551
552
553
554
555
556
557
558
559
560
561

Therefore, a current high-resolution IMS resolving power of 200 is roughly equivalent to a chromatographic efficiency of >200,000 theoretical plates.

Peak capacity of IMS-MS

Complex samples require high efficiency to achieve separation and, even in early stage drug discovery, having a high efficiency affords a good opportunity to separate degradants and process impurities away from the desired product. Peak capacity is defined as the maximum number of peaks that can fit in any two-dimensional method (Ruotolo et al., 2002a). A two-dimensional method will have a high peak capacity if the resolution of each dimension is high and the difference in their separation mechanism (orthogonality) is high. The peak capacity will also be defined by the complexity of the sample and the properties of the analytes in the sample. For example, complex biological samples with a range of retention times will provide larger peak capacities for a technique than that of the analysis of a mixture of analytes of a specific class. Peak capacity is therefore a better, but highly molecule dependent, indicator of the separation power compared to measuring resolution alone.

In an ideal situation the peak capacity of a two-dimensional method is the product of the first and second dimensions (Li et al., 2009), but corrections can be made for cases where the two dimensions are not 100% orthogonal. Whilst the separation based on their size to charge ratio (Ω/z for IMS) and mass to charge (m/z for MS) ratio is, to some extent, orthogonal there is a well-known correlation between mobility (\propto size) and mass (Griffin et al., 1973), as illustrated in Figure 12.



562
563
564
565
566
567

FIGURE 12. Published mass mobility curves showing correlation between reduced mobility and mass within classes, but poor correlation in heterogeneous sets, adapted from Griffin et al. (1973).

Therefore the corrected peak capacity, P_c , in IMS-MS can theoretically be estimated (Dwivedi et al., 2010) using the relationship:

568
569
570
571
572
573
574
575
576
577
578
579
580
581
582
583
584
585
586
587
588
589
590

$$P_c = R_{IMS} \times R_{MS} \times \text{fraction of orthogonality} \quad (8)$$

where R_{IMS} is the average resolving power of the ion mobility spectrometer, and R_{MS} is the average resolution of the mass spectrometer.

An example of increased peak capacity in IMS-MS was observed in a study of various classes of metabolites in blood (Dwivedi et al., 2010) including amino acids, organic acids, fatty acids, purines etc) using a DT-IMS-MS system. In the mass range of 23 – 830 m/z, the drift time spread of ~14.3 ms results in ~28% of the total 2D space, or an average deviation in drift time of ±14% along the theoretical trend. With an average IMS resolving power of 90, average MS resolution of 1500, and ±14% orthogonality, the estimated peak capacity, P_c , for the instrument is $90 \times 1500 \times 14\% = 18,900$. The relatively low MS resolution of 1500 (peak width is 0.27 Da at an average mass value of 404 m/z) in this study (Dwivedi et al., 2010) resulted in an estimated peak capacity of MS alone of 2989. A six fold increase in the peak capacity was therefore observed (~19,000) in IMS-MS compared to MS alone (~3000).

Reverse phase chromatographic columns are routinely used to separate small molecules and the peak capacity for gradient elution high performance liquid chromatography was found to be typically up to 300 (Guo et al., 2009), and up to 400 (Wren, 2005) for gradient elution ultra-performance liquid chromatography. Comparing the peak capacity for different types of IMS with typical traditional chromatography peak capacities (Table 3) shows that the extra dimension of IMS is potentially a powerful separation tool.

591 **TABLE 3.** Approximate separation peak capacity for various analytical separation methods*.

Technique	Approximate peak capacity
<i>FAIMS</i>	<i>8.9-44 (Canterbury et al., 2008)(Schneider et al., 2010b)</i>
<i>DT-IMS</i>	<i>90 (Dwivedi et al., 2010)</i>
HPLC	300 (Guo et al., 2009)
UHPLC	400 (Wren, 2005)
MS	3000 (Dwivedi et al., 2010)
<i>IMS-MS</i>	<i>19000 (Dwivedi et al., 2010)</i>
LC-MS	900000
<i>LC-IMS-MS</i>	<i>11340000 (Dwivedi et al., 2010)</i>

*Ion mobility and hyphenated techniques are italicized

592
593
594
595
596
597
598
599
600
601
602
603
604
605
606
607
608
609
610
611
612
613
614
615

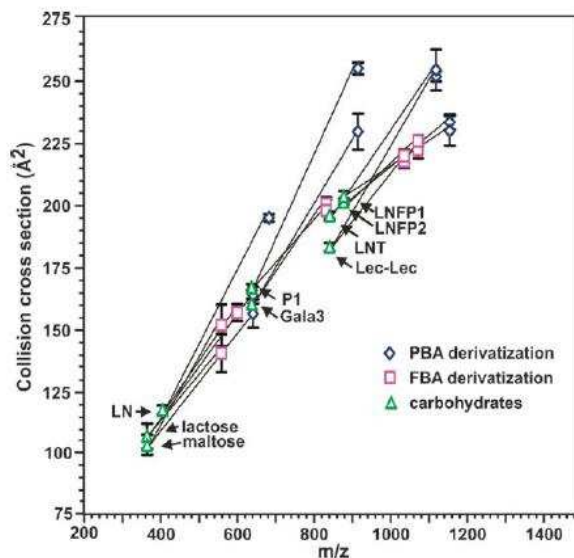
It is conceivable that LC-IMS-MS may become a standard addition or replacement for LC-MS systems due to the ease of configuration and the increase in separating power. Indeed many proteomic applications are increasingly using LC-IMS-MS to separate complex peptide mixtures, leading to unprecedented extensive proteome maps (Liu et al., 2007b; Taraszka et al., 2005). LC-IMS-MS often does not require careful configuration, demanding sampling rates and does not appear to suffer from robustness issues compared to many two-dimensional techniques such as LCxLC, GCxGC etc.

Modifying selectivity in IMS

The selectivity of ion mobility can be modified by increasing the electric field in DT-IMS (Wu et al., 1998), the use of covalent shift reagents (Fenn and McLean, 2008) to derivatise or non-covalent shift reagents (Clowers and Hill, 2006; Howdle et al., 2009) to form complexes with analytes and effect a selective shift in ion mobility relative to coincident analytes, using drift gas modifiers (Fernández-Maestre et al., 2010a) sometimes called clustering agents in DMS-MS (Schneider et al., 2010b)), by altering the composition of the drift gas (Matz et al., 2002) and by the use of different reagent gases in GC-IMS-MS (Eiceman et al., 1995). Currently there does not appear to be a consensus on useful and well characterised selectivity modifiers so method development is presently not fully predictable; however some of these changes are trivial and can be considered analogous to changing the stationary or mobile phases in liquid chromatography.

The use of covalent shift reagents (Fenn and McLean, 2008), as shown in Figure 13, effectively derivatises molecules, potentially creating lower density analogues of the precursor species with a marked increase in the collision cross-section relative to a smaller increase in mass. This is clearly

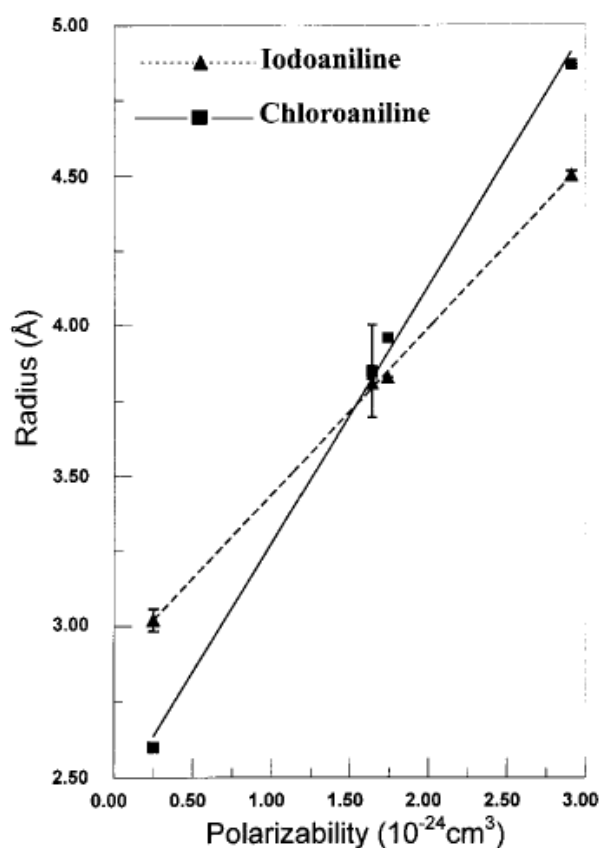
616 illustrated by deviations to larger cross sections compared to the general trend in mass-mobility
 617 correlation for carbohydrates. Compared to the underivatized species it was reported that covalent
 618 derivatisation afforded three distinct advantages: (i) tuneability was increased for isobaric species
 619 difficult to identify and/or resolve by mass spectrometry alone, (ii) an enhanced sensitivity of 2x more
 620 signal intensity was observed and (iii) the derivatised species could be used as tags or fragment
 621 labels in CID and as IR active species in IRMPD studies.
 622



623
 624 **FIGURE 13.** Effect of derivatisation of carbohydrate species with boronic acid on CCS, adapted from
 625 Fenn and McLean (2008).

626
 627 For small molecules the effect of the dipole interaction is typically far more significant than for large
 628 molecules (>500 Da) so that using drift gas modifiers or mixtures can be a powerful method to alter
 629 selectivity (elution order of analytes). Indeed for small molecules such as amino acids the polarisability
 630 has been found to be a critical factor affecting separation of analytes, whereas in large molecules the
 631 collision cross section term dominates (Steiner et al., 2006). Thus for small molecules exploiting
 632 polarizability to probe structural details and maximize separation has immense future potential.
 633

634 An example of the potential of exploiting polarizability to separate analytes is given by the different
 635 slopes of calculated ion radii for iodoaniline and chloroaniline with different drift gases, helium (0.205
 636 $\times 10^{-24}$ cm³), argon (1.641×10^{-24} cm³) and carbon dioxide (2.911×10^{-24} cm³), indicating that it should
 637 be possible to separate any analytes with different slopes (Figure 14) by choosing an appropriate drift
 638 gas composition.



639
640

641 **FIGURE 14.** Calculated ion radii as a function of drift gas polarizability, from Asbury & Hill, 2000c.

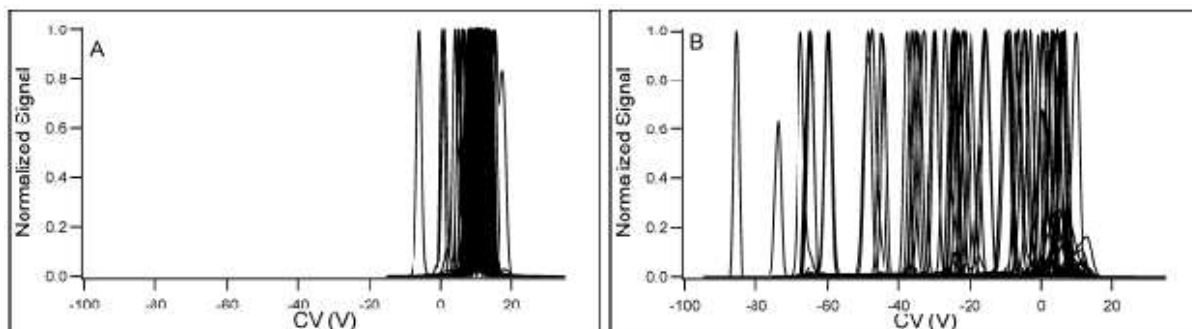
642

643 The use of vapour modifiers added to the drift gas in planar DMS-MS has been widely explored (e.g.
644 Levin et al., 2007 and Eiceman et al. 2004) , although the full mechanism of the interactions has not
645 been elucidated enough to enable predictable separations in mixtures. Levin et al. (2004)
646 systematically examined the effect of various polar clustering agents and postulated strong effects
647 due to hydrogen-bonding potential, electrostatic attraction, steric repulsion and energetically feasible
648 conformations. A series of publications exploring the cluster/declustering (Krylov et al. 2002, Krylov et
649 al. 2009, Schneider et al. 2010a, Schneider et al. 2010c, Coy et al. 2010) further explored the
650 possibility of predicting analyte shifts in response to changes in drift gas modification and provide a
651 powerful route to optimising separations.

652

653 The 'cluster/declustering effect' that addition of vapour modifier induces appears to have dramatic
654 effects on the peak capacity in a planar electrode configuration (Schneider et al., 2010b), improving
655 the peak capacity for a 70 component mixture from 13 in pure nitrogen to 44 in 2-propanol doped
656 nitrogen (see FIGURE 15), although this had the disadvantage that 10/70 components were depleted
657 in intensity by 20-fold or more due to them having a lower proton affinity than the dopant.

658

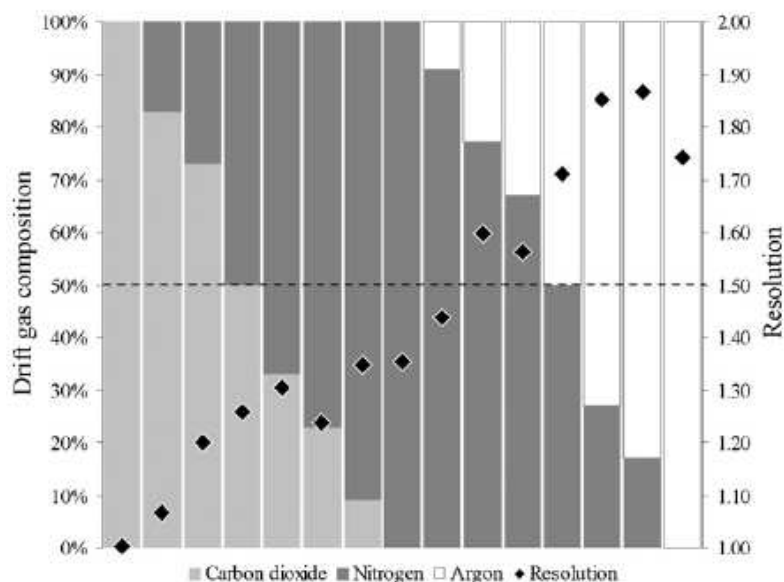


659

660 **FIGURE 15.** Separation of a 70-compound mixture with (A) nitrogen transport gas and (B) nitrogen
 661 with 1.5% 2-propanol in parallel plate FAIMS configuration, adapted from Schneider et al., (2010b).

662

663 Changes to the temperature, composition (Beegle et al., 2001) and pressure of a single drift gas is
 664 commonly used to change selectivity and IMS gasses including nitrogen, air, helium, carbon dioxide
 665 and sulphur hexafluoride have been evaluated. The use of binary gas mixtures (Howdle et al., 2010),
 666 shown in Figure 16, results in excellent selectivity enhancements over single gas composition IMS
 667 separations and demonstrates that this selectivity is tunable by altering the binary gas composition.
 668



669

670 **FIGURE 16.** Effect of drift gas composition on the ion mobility resolution of the drugs rosiglitazone
 671 and lamotrigine $[M+H]^+$ ions in binary drift gas mixtures in TWIMS. The composition of the binary drift
 672 gas mixtures are represented by shaded bars indicating the percentage of each gas in the mixture
 673 (left hand axis). Resolving powers greater than 1.5 indicate full separation of components and this
 674 threshold is indicated by the dashed line at a resolution of 1.5. The resolution of lamotrigine and
 675 rosiglitazone is indicated by the right hand axis. Adapted from Howdle et al., (2010).

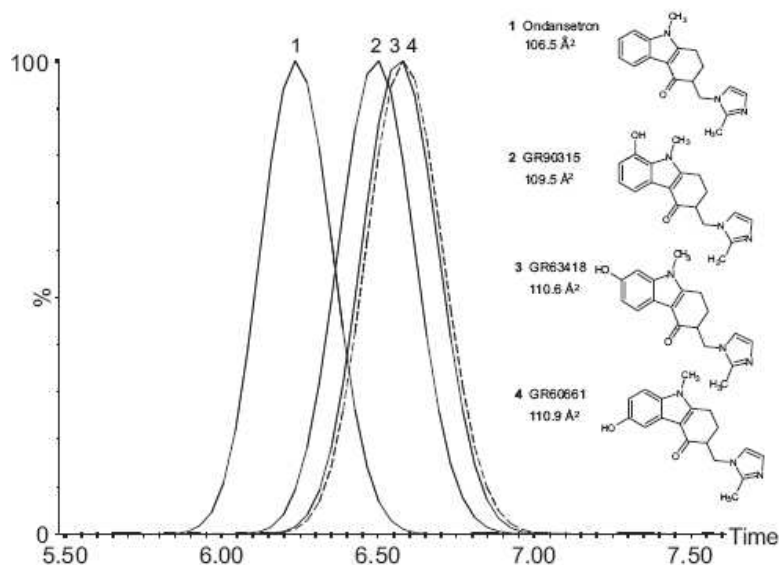
676

677 **IV. APPLICATIONS OF IMS AND IMS-MS SEPARATIONS IN SMALL** 678 **MOLECULE ANALYSIS**

679 IMS has been investigated for the analysis of a wide range of small molecule applications including
 680 active pharmaceutical ingredients (Budimir et al., 2007; Karimi and Alizadeh, 2009; O'Donnell et al.,
 681 2008; Wang et al., 2007) veterinary drugs (Jafari et al., 2007), metabolites (Alonso et al., 2008),
 682 pesticides (Jafari, 2006; Keller et al., 2006; Tuovinen et al., 2000), prescription and illicit drugs (Dussy
 683 et al., 2008; Lawrence, 1986), combinatorial libraries (Collins and Lee, 2001), autonomous health
 684 diagnostics (Zhao et al., 2010) and immunoassay detection (Pris et al., 2009; Snyder et al., 1996).
 685 Here we outline some highlights of small molecule analysis using IMS-MS systems.

686 **A. Low abundance metabolite and small molecule identification using IMS-MS**

687 A novel use of LC-IMS-MS was demonstrated for a 5HT₃ antagonist, ondansetron, and its aromatic
688 hydroxyl isomeric metabolites (Dear et al., 2010) that are typically generated *in vivo* and *in vitro*.
689 Using conventional UHPLC-MS-MS the unambiguous characterisation of the hydroxyl metabolites
690 would not be possible as they can produce identical MS/MS spectra. Using UHPLC-MS in a biological
691 matrix system ondansetron and metabolites display different retention times but could not be
692 assigned without using purified standards as a reference. Using an IMS separation, shown in Figure
693 17, and *in silico* methods the components were identified based on their ion mobility. For these
694 components a low number of rotatable bonds are present so the computational method is rapid,
695 interpretation of complex NMR spectra is not required and isolation or synthesis is unnecessary to
696 create primary standards. In this case the identity of metabolites with smaller than 1 Å² difference
697 between their CCS was distinguished using a combination of Waters Synapt TWIMS by comparison
698 with CCS values obtained using computational methods.

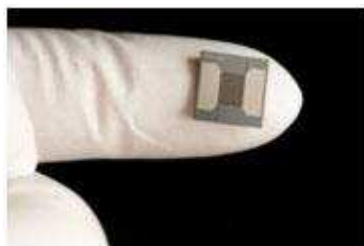


699 **FIGURE 17.** TWIMS ion mobility arrival time distributions for ondansetron and the 6-, 7- and
700 8-hydroxyl metabolites, adapted from Dear et al., (2010).
701

702 The subsequent use of product ion mobility as a tool for assignment of positional isomers (Cuyckens
703 F et al., 2011) was also demonstrated for both model compounds and a real-case example,
704 emphasizing the possibilities of structural determination by both parent ion and product ion mobility
705 where mass spectra alone appear indistinguishable and cannot be used to confidently assign a
706 candidate structure. For example two different product ion mobilities for 11 *ortho*, *meta* and *para*
707 substituted hydroxyl metabolites with a phenylethylamine substructure were sufficient to assign their
708 structures.

709 **B. Rapid, portable and sensitive analysis using miniaturisation of IMS and IMS-MS**

710 One of the advantages of FAIMS is that it does not require complicated vacuum equipment or large
711 analyser tubes, thus it may be easily hyphenated to a portable mass spectrometer system (Manard et
712 al., 2010). Microfabricated FAIMS chips can increase the speed of separation by 100-10,000 times,
713 filtering ions on the microsecond timescale enabling rapid monitoring of species at low level
714 concentrations (Shvartsburg et al., 2009a). Whilst the current microfabricated FAIMS units, example
715 shown in Figure 18, are more suited to distinguish compound classes than individual species the
716 multichannel FAIMS electrodes enables integration with an air sampler, ionisation source and
717 detector for applications such as gas analysis, chemical monitoring and autonomous health
718 diagnostics (Zhao et al., 2010).
719



720

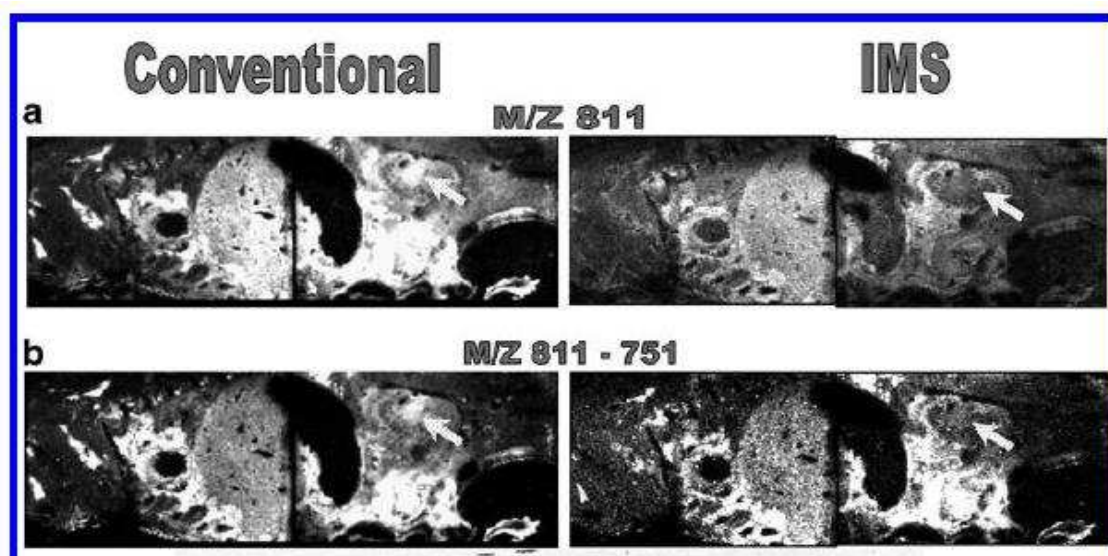
721 **FIGURE 18.** Illustration of the size of microfabricated FAIMS chip, courtesy of Owlstone
722 Nanotechnologies and Pacific Northwest National Laboratory.

723 **C. Increased selectivity in ambient and surface analysis mass spectrometry using IMS-MS**

724 The direct and rapid analysis of substances using ambient ionisation mass spectrometry sources
725 allows mass spectrometry data to be obtained with little or no sample preparation required for a
726 variety of surfaces and matrices from tissue samples to intact tablet or liquid formulations. Application
727 areas have included quantitative and qualitative measurements in pharmaceutical analysis, forensics,
728 bioanalysis, *in vivo* imaging, proteomics etc. Whilst MALDI has been widely adopted in biological
729 applications, for the analyses of biomolecules, there is currently a great deal of interest in ambient
730 mass spectrometry approaches and there are now at least thirty methods documented (Weston,
731 2010).

732

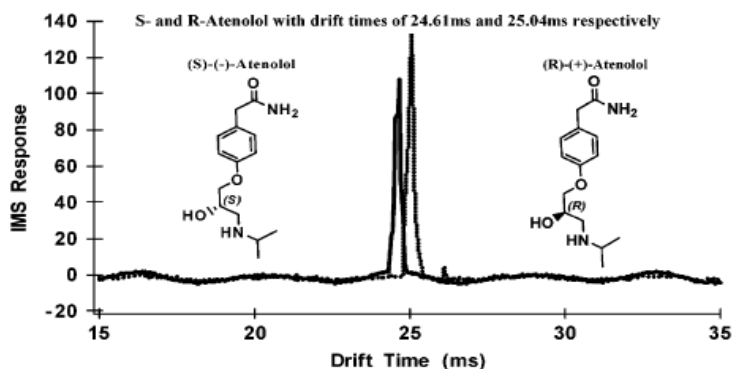
733 The introduction of an additional IMS stage adds a further separation step to ambient mass
734 spectrometry analysis without the need for rigorous sample preparation. Indeed for most surface
735 analysis mass spectrometry methods the fact that the surface is sampled and ions are generated in a
736 single step means that the only viable method of separation and selectivity before the mass detector
737 is to use a gas-phase separation method such as IMS. This extra selectivity maybe particularly useful
738 in imaging applications. In the case of the example of whole-body imaging of rats, the rats were dosed
739 with 6 mg/kg *iv* with the anticancer drug vinblastine and the removal of interfering isobaric ions from
740 endogenous lipids helps increase confidence in the MALDI imaging data (Jackson et al., 2007) by
741 removing 'false positives' which, by mass spectrometry imaging alone, could be interpreted as
742 containing a high concentration of the active drug, as shown in Figure 19. The extra dimension of
743 separation could also prove useful in removing any matrix-related isobaric ions. The datasets from the
744 Driftscope imaging platform were transferred to Biomap 3.7.5.5 for visualization enabling facile
745 interpretation.



746
 747 **FIGURE 19** . MALDI-IMS-MS image showing distribution of ions in whole-body sections and the
 748 arrow points to the area where specificity increased with application of IMS, adapted from Jackson et
 749 al., (2007).
 750

751 **D. Chiral analysis using IMS-MS**

752 A chiral modifier at 10 ppm of (S)-(+)-2-butanol was added to the buffer gas and enantiomers of a
 753 β -blocker, atenolol, were separated (Dwivedi et al., 2006), as shown in Figure 20. It is proposed that
 754 selective interactions occur in the gas-phase between the enantiomer ion and the chiral modifier, to
 755 temporarily form a diastereomeric pair, so that the mobilities of the enantiomers are altered and can
 756 be separated in time. Chiral ESI-DT-IMS-MS is now commercialised via the Excellims Corp IMS-
 757 quadrupole-MS system. A smaller, portable chiral IMS detector is now being developed by Excellims
 758 Corp for fast, on-site analysis including pesticide residues and environmental samples (Anon). The
 759 advantages of chiral IMS-MS compared to competing analytical techniques such as chiral SFC and
 760 chiral HPLC include rapid method development and high sensitivity, enabling rapid determination of
 761 enantiomeric excess (e.e.) for use in QA/QC environments or in broader applications including
 762 biomarker and metabolite identification.



763
 764
 765 **FIGURE 20**. DT-IMS-MS separation of atenolol enantiomers showing the superimposed spectrum of
 766 the R and S enantiomers (similar results obtained using racemic mixture, not shown). Adapted from
 767 Dwivedi et al., (2006).

768 Chiral resolution using FAIMS-MS has also been reported for 6 pairs of amino acid enantiomers
 769 separated as metal-bound complexes of divalent metal ion with an L-form amino acid (Mie et al.,

2007), shown in Figure 21. The method employed a range of additional divalent metal cations and reference amino acids. Screening with different metal cations and reference compounds compares favourably with chiral HPLC and SFC screening times and can be automated using automated sample preparation platforms.

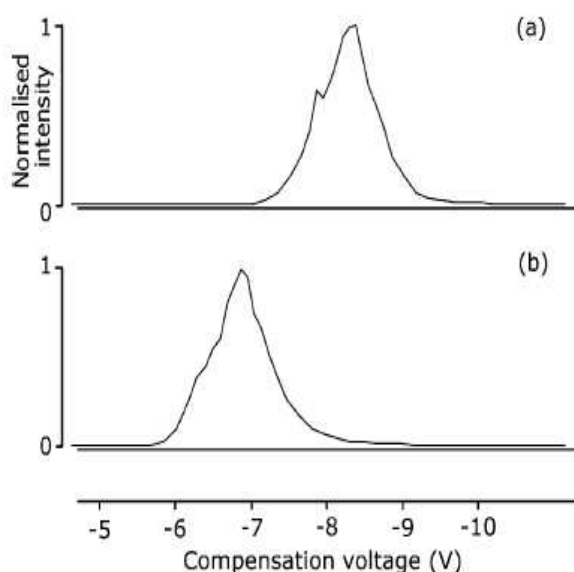
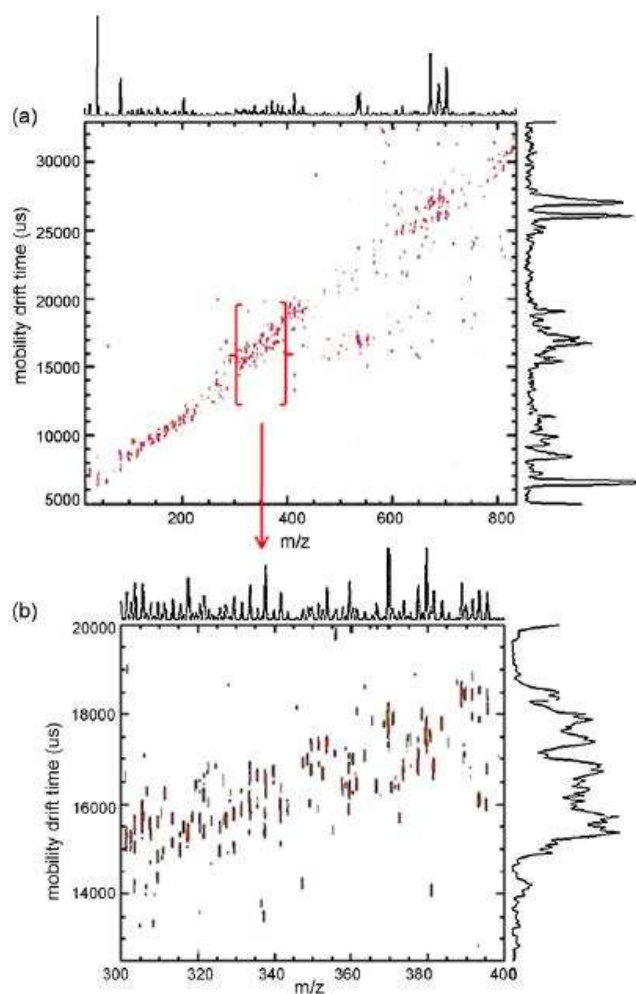


FIGURE 21. Separation of D/L-valine as $[\text{Cu}^{2+}(\text{I-Trp})_2(\text{D/L-Val})\text{-H}]^+$. (a) D-Val; (b) L-Val. Adapted from Mie et al., (2007).

An example of epimer separation where the diastereomers differ by only one chiral carbon, was achieved for betamethasone and dexamethasone (Campuzano et al., 2011). The separation of the two epimers correlated well with differences observed in the calculated B3LYP/6-31G++(d,p) electrostatic potential surface. Whilst baseline separation is achievable by HPLC (Arthur et al., 2004) the mass spectra of these compounds is very similar so the rapid separation and correlation with molecular modeling quickly identify this pair of compounds.

E. Resolution of isobars and isomers in complex mixtures using IMS-MS

Over 1100 metabolites were detected from methanolic extracts of 50 ul of blood samples including separation of over 300 isobaric/isomeric components, achieved without pre-concentration (Dwivedi et al., 2010), shown in Figure 22. The peak capacity compared to mass spectrometric analysis alone was increased by ~6 times and a broad range of metabolites were detected including lipids, carbohydrates, isoprenoids and estrogens. Interpretation of the data is further enabled by examining characteristic mobility-mass correlation data to identify similar classes of metabolites. In addition a reduction in the background noise due to selective ion filtering enabled detection and identification of low abundance components.



792

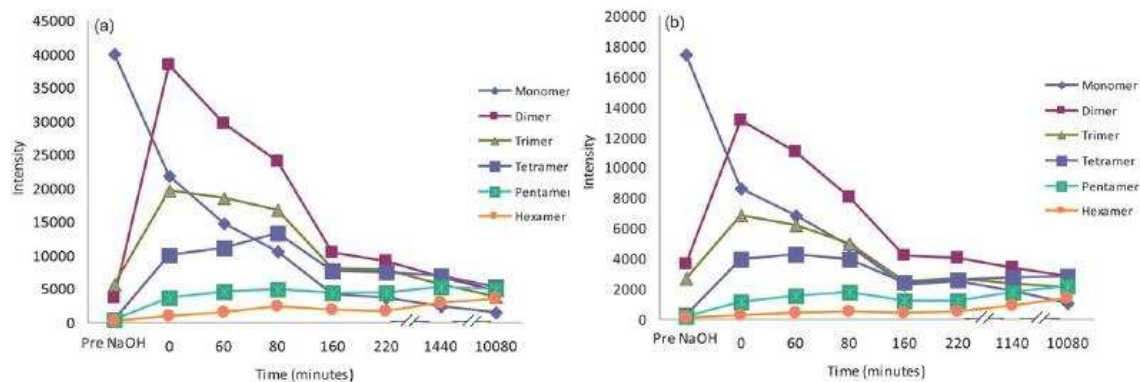
793 **FIGURE 22.** (a) Two-dimensional spectra of metabolic features measured in methanolic extract of
 794 human blood (b) a zoomed in region of the DT-IMS-MS spectrum illustrating peaks detected at the
 795 same nominal mass with different mobilities showing separation of isomers and isobars, adapted from
 796 Dwivedi et al., (2010).

797 **F. Real-time reaction monitoring and process monitoring using IMS-MS**

798 Reaction-monitoring in real-time has the potential to enable understanding of when reactions can be
 799 terminated at a suitable, rather than arbitrary, endpoint. By monitoring a process regularly throughout
 800 the reaction time knowledge may also be accrued of the reaction, intermediates and product
 801 formation that could not be understood by irregular, sparse sampling alone and enable optimization of
 802 experimental parameters via chemometrics. The products formed by deprotonation of 7-fluoro-6-
 803 hydroxy-2-methylindole with sodium hydroxide were monitored by TWIMS-MS (Harry et al., 2011) and
 804 showed complementary and extra information from TWIMS-MS compared to MS alone with shape
 805 selectivity information obtained by sampling every several minutes over a timescale of several hours
 806 (Figure 23).

807

808

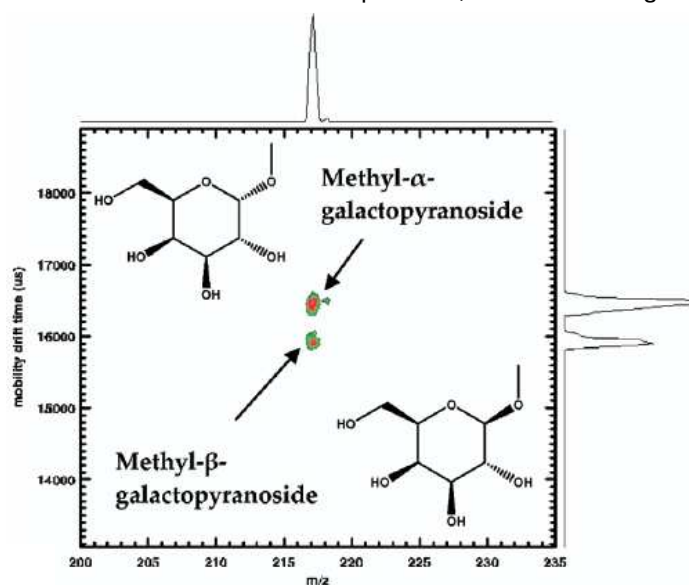


809

810 **FIGURE 23.** MS and TWIMS-MS analysis of the reaction of 7-fluoro-6-hydroxy-2-methylindole
 811 following the addition of aqueous sodium hydroxide. Signal response versus time in minutes for m/z
 812 166 (monomer, I), m/z 311 (O-linked dimer, II), m/z 456 (O-linked trimer), m/z 601 (O-linked tetramer),
 813 m/z 746 (O-linked pentamer) and m/z 891 (O-linked hexamer) using (a) MS and (b) IM-MS. Adapted
 814 from Harry et al., (2011).

815 G. Rapid resolution of carbohydrate isomers using IMS-MS

816 Carbohydrate isomers including oligosaccharides are involved in numerous biological processes,
 817 such as cell-cell recognition and the development of embryos, but one of the main functions of
 818 carbohydrates is as oxidisable substrates in catabolism. However, to fully understand their different
 819 roles and functions we need to understand both the linkage type and anomeric configuration whilst
 820 dealing with the challenge that, for example, in a mixture of 16 D and L-aldohexoses and 8 D and L-
 821 aldoses the total number of isomers with the same mass will be 96. The use of mass spectrometry as
 822 a tool is hindered by the similarity between fragmentation data obtained for different isomers; however
 823 purification and determination of purity by NMR requires interpretation time and larger amounts of
 824 material. Separation of the metal ion adducts of anomeric methyl glycoside isomers (MeMan, MeGal
 825 and MeGlc) and isomeric forms of reducing sugars (Dwivedi et al., 2007), branch isomers, and very
 826 closely related isomers varying at a single stereochemical position (Zhu et al., 2009) were addressed
 827 where MSⁿ was not able to deliver solutions to the problem, as shown in Figure 24.



828

829 **FIGURE 24.** Two-dimensional DT-IMS-MS spectra of a mixture of methyl-α and β-D-
 830 galactopyranosides showing the separation (N₂ drift gas) of the sodium adducts at m/z 217, adapted
 831 from Dwivedi et al. (2007).

832

833 H. Rapid analyte testing in complex drug formulations by IMS-MS

834 The combination of IMS-MS with ambient ionisation mass spectrometry may enable rapid analysis for
835 complex mixtures including drug formulations without laborious method development and
836 consumables required by other separation methods such as 2D LC-MS etc.

837 The complementary techniques of IMS and DART ambient ionisation operated separately has been
838 demonstrated for AG-013736 in 1 mg Axitinib tablets (Likar et al., 2011), enabling a rapid analysis of
839 AG-013736 in AG-013736 drug substances by DART ionisation and analysis of low-level limits for
840 absence of the drug in placebo tablets by ion mobility spectrometry using a Model 400B IONSCAN-LS
841 from Smiths Detection Scientific (Danbury, CT).

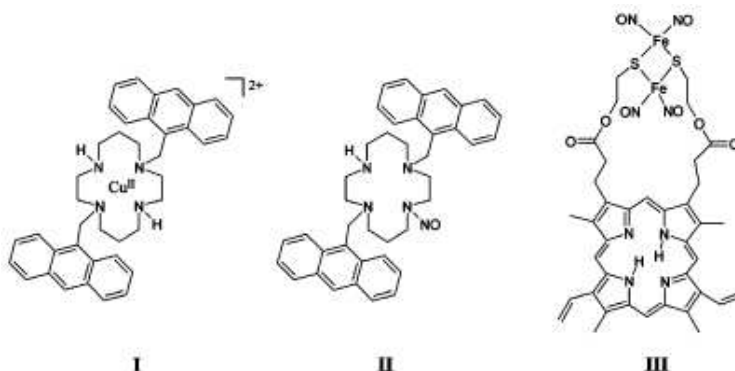
842 Hyphenated ambient ionisation IMS-MS and nano-electrospray has been used to analyse:

- 843 • pharmaceutical formulations including tablets and creams containing one or more of ranitidine,
844 paracetamol, codeine, anastrozole chlorhexidine and a nicotine-containing skin patch (Weston et
845 al., 2005) using DESI.
- 846 • pharmaceutical formulations from tablets containing one or more of timolol, paroxetine,
847 paracetamol and codeine using nano-electrospray ionisation (Budimir et al., 2007).
- 848 • pharmaceutical formulations containing one or more of paracetamol, ephedrine, codeine and
849 caffeine from non-bonded reversed-phase thin layer chromatography (RP-TLC) plates by
850 desorption electrospray ionisation (DESI) (Harry et al., 2009).

851 These examples demonstrate the wide applicability of analyses in various types of formulation
852 illustrating that pre-treatment of samples is not required, rapid analyses can be conducted, whilst
853 maintaining reproducible and robust results.

854 I. Analysis of supramolecular complexes using IMS-MS

855 The syntheses of supramolecular complexes that possess photo-optical properties are desired for
856 solar energy capture and conversion, molecular machines, photochemical drugs and fluorescent-
857 based sensors.

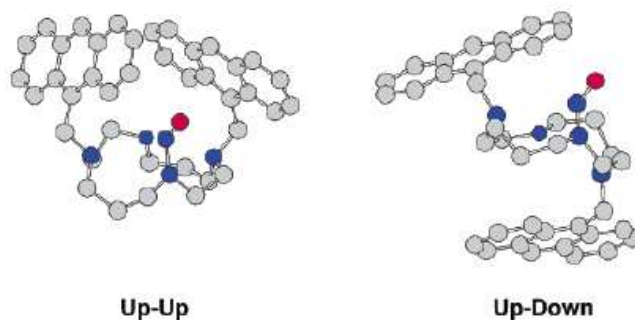


858
859 **FIGURE 25.** Schematic of $\text{Cu}^{2+}(\text{DAC})^{2+}$ (I), DAC-NO (II), and PPIX-RSE (III), adapted from Baker et
860 al., (2005).

861 DT-IMS-MS was used to probe the structures of bichromic complexes (Figure 25; Baker et al., 2005)
862 in order to provide relevant data for sampling from *in situ* fluid data. Complementary data to $^1\text{H-NMR}$,
863 x-ray crystallography and fluorescence measurements were obtained.

864 For I the crystal structure agreed well with DFT structures and IMS-MS measurements, indicating that
865 solid-state structures agreed well with gas-phase measurements. Only a single peak was observed in
866 the ion mobilogram and calculation gave 161 \AA^2 as the CCS, compared to $166 \text{ \AA}^2 \pm 5 \text{ \AA}^2$ predicted
867 from the DFT structure.

868 For II DT-IMS-MS measurements indicated two conformers by observation of two main bands in the
869 ion mobilogram, by comparison with computational data this suggested two major families of Up-Up
870 and Up-Down configuration, as shown in FIGURE 6. The solution NMR data for II also suggested two
871 conformers but the structures could not be unambiguously determined from the data.

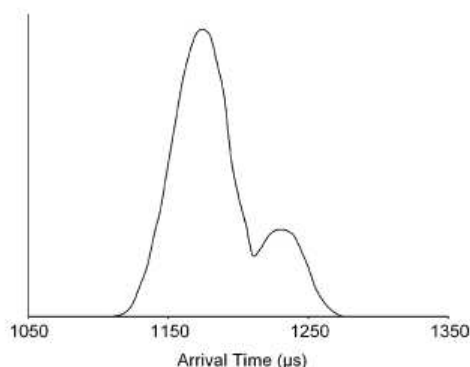


872

873 **FIGURE 26.** Examples of the two families predicted for $(II + H)^+$. The Up-Down family is the lower
 874 energy family, the Up-Up family has both anthracenyl groups on the same side as the cyclam.
 875 Adapted from Baker et al., (2005).

876

877 For III DT-IMS-MS measurements indicated two conformers which, in combination with DFT
 878 measurements indicated two compact structures, rather than folded structures, and correlated well
 879 with photophysical features including a bimodal fluorescent decay and a residual emission in steady-
 880 state luminescence experiments. The proportion of the two conformers measured by IMS-MS, shown
 881 in Figure 27, agreed well with pre-exponential factors that indicated an approximate 80:20 ratio.



882

883 **FIGURE 57.** ATD for $(III + H)^+$ obtained at 80 K. Two distinct peaks indicate two conformers of
 884 $(III + H)^+$ are present, adapted from Baker et al., (2005).

885 **J. Hydration and desolvation of ligands and substrates**

886 In drug design it is important to consider water molecules particularly in two situations:

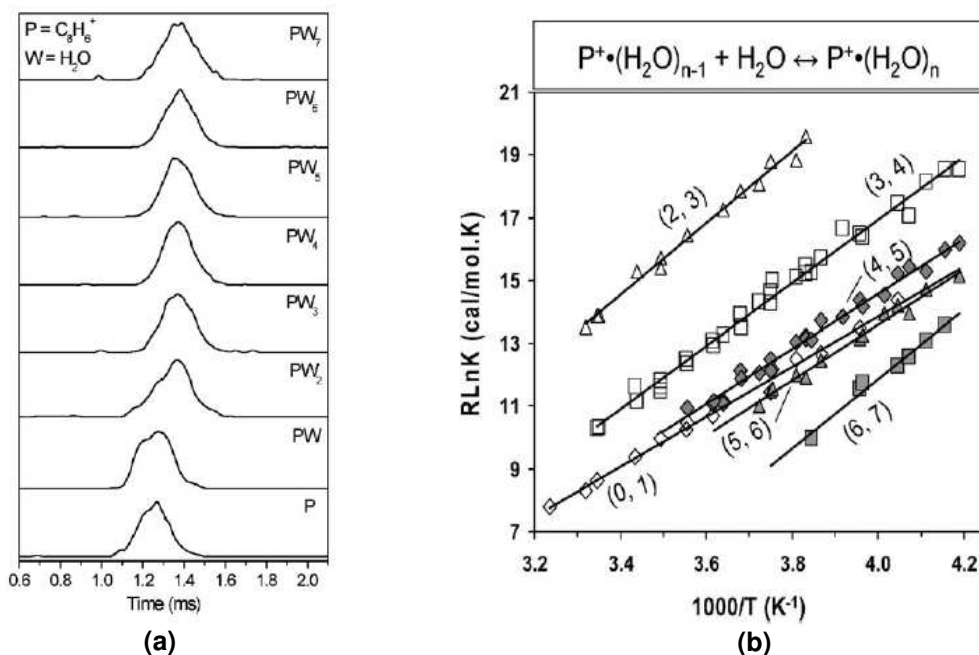
- 887 (i) those water molecules that will be displaced during ligand binding in a receptor (Poornima
 888 and Dean, 1995), and
- 889 (ii) those water molecules that will be desolvated crossing the membrane environment.

890

891 Water in binding pockets in a receptor can provide surprising entropic and enthalpic contributions to
 892 structure and binding affinities (Pace et al., 2004; Homans, 2007). If the key water binding sites and
 893 influence of 'small molecule' ligands are known it may be possible to use this information in medicinal
 894 drug design, or to predict static hydration sites. It may be especially important to consider bridging
 895 waters that link ligand to protein via an extended hydrogen bond network.

896

897 Understanding membrane permeability is key to drug delivery and activity and is typically understood
 898 by hydrogen bond descriptors such as polar surface area (PSA) and surrogate measurements such
 899 as logD. These are considered important physicochemical parameters and modulated during lead
 900 optimisation. The reason that these parameters are important is that it is polar groups that are most
 901 involved in desolvation when molecules move from an aqueous extracellular environment to the
 902 lipophilic membrane environment. During this migration molecules may change their conformation
 903 and lose water molecules in order to cross the membrane barrier. To further understand the effect of
 904 desolvation on ligands it is possible to add/remove water molecules one by one by changing the water
 905 vapour pressure of the DT-IMS-MS cell and gradually ascertain the ion mobility and conformation
 906 adopted from a hydrated towards a non-hydrated ion, shown in Figure 28(a). By measuring the
 907 energy change at different temperatures a van't Hoff plot can be generated, shown in Figure 28(b),
 908 thereby revealing the entropic and enthalpic contributions to hydration.



910 **FIGURE 28.** (a) ATDs of hydrated phenyl acetylene ions (PW_n) obtained following the injection of the
 911 phenyl acetylene ion ($C_8H_6^{\bullet+}$) into 0.34 Torr of water vapor at 249 K (b) Van't Hoff plots for the
 912 equilibria $C_8H_6^{\bullet+}(H_2O)_{n-1} + H_2O \rightleftharpoons C_8H_6^{\bullet+}(H_2O)_n$ for $n-1$ and n as indicated. Adapted from Momoh &
 913 El-Shall., (2008).

914
 915 Hydration of small molecules has been studied for the phenyl acetylene ion, with stepwise hydration
 916 energies of $39.7 \pm 6.3 \text{ kJ mol}^{-1}$ from $n=1$ to 7; the entropy change for step 7 is larger, indicating a
 917 cyclic or cage like water structure (Momoh & El-Shall, 2008). For the benzene ion stepwise hydration
 918 energies were 35.6 kJ mol^{-1} from $n=1$ to 6. The binding energies were larger in the $n=7$ and 8 clusters
 919 indicating cyclic or cage like water structures (Ibrahim et al., 2005). For small protonated peptides the
 920 hydration energy is largest for highly charged peptides and small non-arginine containing peptide and
 921 typically 30 to 60 kJ mol^{-1} (Wyttenbach et al., 2003); for pentapeptides AARAA, AARAA-OMe and Ac-
 922 AARAA the binding energies were typically $\sim 41 \text{ kJ mol}^{-1}$.

923
 924 The foregoing IMS-MS studies indicate hydration/desolvation studies of small molecule ions can
 925 provide structural information in the gas phase, this may be relevant to:

- 926 1) understanding water and hydrogen bonded networks (including their entropic consequences)
 927 involving protein, ligand and water as part of molecular recognition systems,
 928 2) ligand desolvation on transport through membrane environments, and
 929 3) hydrogen/deuterium exchange experiments and how they are effected by molecular
 930 conformation.

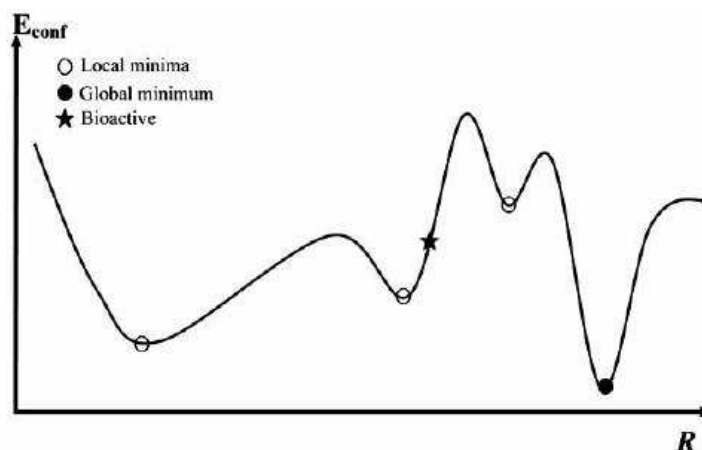
931
 932 Other methods to measure the hydration of small drug-like molecules include infra-red data recorded
 933 from a hydrated electrospray source or a droplet ion source (Pouilly et al., 2008) but these have not
 934 always provided unambiguous data, possibly due to the lack of energy required for proton transfer.
 935 The measurement of hydration/desolvation energies, described above, may provide a unique insight
 936 into the energy landscape of hydration/desolvation by conducting measurements over a range of
 937 temperatures.

938 V. OVERVIEW OF COLLISION CROSS-SECTION (CCS) MEASUREMENTS FOR SMALL 939 MOLECULES

940
 941 In DT-IMS-MS and TWIMS-MS, larger ions (with a larger CCS) tend to migrate slower through the
 942 gaseous medium in the IMS cell compared to smaller ions due to a higher number of collisions with
 943 the gas molecules (typically an inert gas such as nitrogen). The drift times through the IMS cell can
 944 also reveal structural information such as size, shape and topology; potentially including information

945 relating to accessible conformations. Unfortunately DMS and FAIMS are, currently, not suitable for
946 carrying out CCS measurements.

947
948 Understanding small molecule structure in the gas-phase may be advantageous for quality control or
949 for a more detailed understanding of molecular structure in the gas-phase. For example in drug
950 discovery the physicochemical and binding properties of small molecules depend on their 3D
951 structure and at physiologically relevant temperatures a conformationally flexible small molecule is
952 expected to be able to access a number of energetically feasible conformers, an example is shown in
953 Figure 29. The timescale of interconversion of conformers will define the structural information that
954 can be obtained in solution and in the gas-phase. Understanding the energetics of small molecule
955 conformers is currently largely carried out by generating potential conformers, known as
956 conformational sampling, in computational studies (Foloppe & Chen, 2009).



957
958 **FIGURE 29.** Hypothetical example of a one-dimensional molecular conformational potential energy
959 surface. Conformational degrees of freedom (R) are shown on the X axis. Adapted from Foloppe &
960 Chen (2009).

961
962 Computationally sampled models have been compared with x-ray crystallographic structures to
963 understand how well the conformer models correlate with the bioactive conformation. Solution NMR
964 can provide valuable information about the 3D structure; however the interpretation is often difficult
965 due to the exchange between several conformations and typically requires molecular modelling to
966 interpret results.

967
968 Rapid calculation of CCS by IMS-MS may be useful to decide which molecules in a library (series)
969 could provide the optimum activity. This could be achieved coarsely by excluding molecules which are
970 too rigid/flexible or too big/small as suggested by Williams et al. (2009a). These experiments
971 potentially have the advantage of rapid speed of experiment and low consumption of sample relative
972 to NMR and x-ray techniques. Understanding the conformation in the gas-phase may be a good
973 indicator of the bioactive conformation. This may be especially relevant to compounds in drug
974 discovery which are challenging to isolate and characterise their structure. Mapping the
975 conformational landscape defined via stereo-centres, intramolecular cyclisation etc., may help
976 uncover a path to identification of new target compounds.

977
978 For protein structures there is now significant evidence that the gas-phase protein structure can
979 reflect the native state solution phase structure under certain carefully controlled conditions. There
980 have been several publications that demonstrate a good correlation between x-ray, NMR and IMS
981 studies for protein structures (Heck and van den Heuvel, 2004; Rand et al., 2009; Ruotolo et al., 2005;
982 Schultz and Solomon, 1961; Shelimov et al., 1997; Shelimov and Jarrold, 1997), although there have
983 also been some differences noted (Jurneczko and Barran, 2011). However for small molecular
984 weight molecules the evidence that gas-phase structures are similar to solution phase structures has
985 been questioned; in a protein there are multiple cooperative interactions that maintain the 3D
986 structure whereas for a small molecule there are typically fewer interactions resulting in a more
987 flexible structure. Furthermore Allen et al. (1996) compared a range of gas-phase and x-ray molecular
988 substructures for small molecules and suggested that high-energy conformers were represented more
989 in gas-phase, room-temperature Boltzmann distributions than in crystal structures and broad peaks

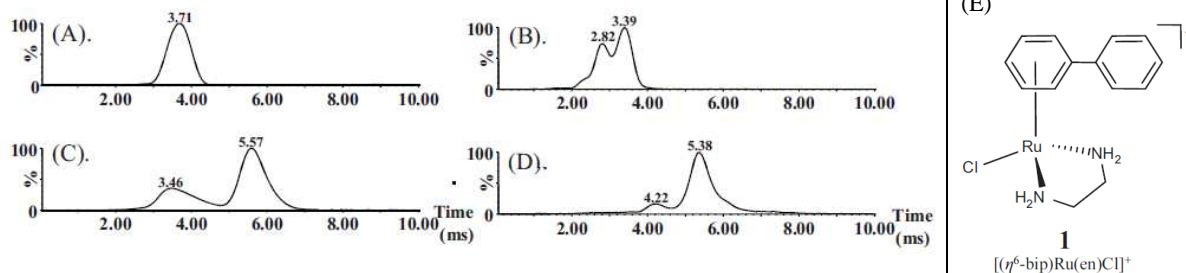
990 observed in IMS have generally been interpreted as indicating that multiple conformations are
991 accessible and interconvert on the IMS measurement timescale.
992

993 Measurements using IMS-MS may not be the same as NMR (which are subject to solvent effects) or
994 x-ray (which are subject to crystal lattice effects). In enzymes and membrane receptors, biomolecular
995 recognition processes are likely to take place in hydrophobic 'binding pockets' of proteins where there
996 will then be several interactions for a ligand including hydrophobic amino acids, with a large possibility
997 (>0.8) of excluding most water molecules. The dielectric constant of a partial vacuum in IMS-MS (c.f.
998 $\epsilon_{\text{vacuum}} = 1$) is more similar to the immediate environment of a membrane receptor ($\epsilon_{\text{peptide/protein}} = 2-4$)
999 than for water ($\epsilon_{\text{water}} = 80$) (Bastug and Kuyucak, 2003). We may therefore postulate that the
1000 environment of a bioactive conformer will often be intermediate between aqueous and gas-phase
1001 (vacuum). Therefore the gas phase may be an appropriate medium in which to study the 'small
1002 molecule' structures which in their active form are bound to a receptor located in a membrane, rather
1003 than in solution.

1004 A. CASE STUDIES OF COLLISION CROSS-SECTION (CCS) MEASUREMENTS FOR SMALL 1005 MOLECULES

1006 1. Study of an organoruthenium complex and its adducts with a DNA oligonucleotide

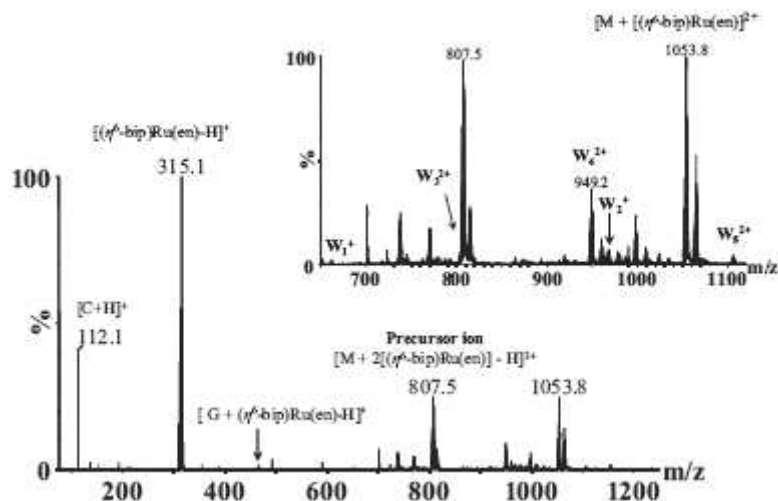
1007 TWIMS-MS has been used to understand the binding of a "piano-stool" shaped organoruthenium
1008 complex with a single stranded oligonucleotide hexamer that show promise as an anti-cancer agent.
1009 The illustration in Figure 30 shows examples of the protonated and deprotonated complexes, the
1010 doubly positive charged complex and the doubly negative charged complex. The single peak (A)
1011 suggests a single species, whereas multiple peaks in (B), (C) and (D) suggest either multiple binding
1012 of the Ru-drug fragment (confirmed by interpretation of the mass spectra collected) or different
1013 conformers present in the mononucleotide due to different charge distributions along the phosphate
1014 backbone (Williams et al., 2009a).
1015



1016

1017 **FIGURE 30.** Arrival time distributions (ATDs) or drift times for (A) the $[\text{M}+2\text{H}]^{2+}$ ion of d(CACGTG); (B)
1018 the $[\text{M}-2\text{H}]^{2-}$ ion of d(CACGTG); (C) the complex $[\text{CACGTG}+2[(\eta^6\text{-bip})\text{Ru}(\text{en})]-2\text{H}]^{2+}$; and (D) the
1019 complex $[\text{CACGTG}+2[(\eta^6\text{-bip})\text{Ru}(\text{en})]-6\text{H}]^{2-}$ and (E) structure of the organoruthenium anticancer
1020 complex ($[(\eta^6\text{-bip})\text{Ru}(\text{en})]$), adapted from Williams et al., (2009a).

1021 The CCS values obtained for the Ru-based drug correlated well with those obtained by x-ray
1022 crystallographic data so that binding could be easily identified. Using MS/MS experiments, shown in
1023 Figure 31, subsequent to IMS separation, enabled the binding site to be determined by examining the
1024 resulting fragmentation pattern.



1025

1026

1027

1028

FIGURE 31. MS/MS spectrum of the precursor ion of m/z 807.5, corresponding to $[\text{CACGTG}+2[(\eta^6\text{-bip})\text{Ru}(\text{en})] \text{H}]^{3+}$. Inset shows the relevant sequence-specific ions detected. (Note: M represents CACGTG), adapted from Williams et al., (2009a).

1029

2. Study of the in-flight epimerisation of a bis-Tröger base

1030

1031

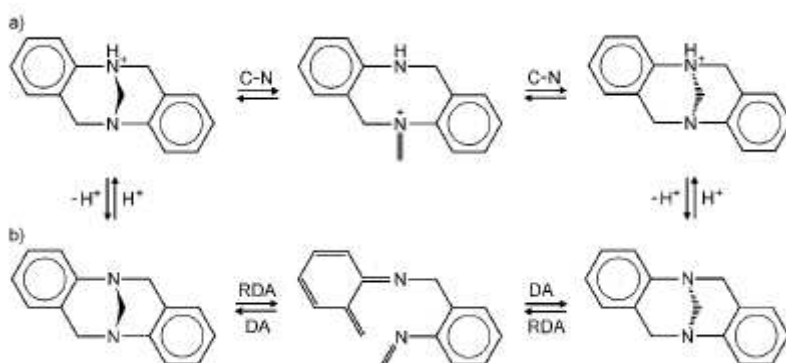
1032

1033

1034

1035

The epimerisation pathway via the proposed alternatives of a) a proton catalysed ring opening or b) retro-Diels-Alder of a bis-Tröger base, shown in Figure 32, were investigated using TWIMS-MS (Révész et al., 2011) as this could be important for the design of Tröger bases which, with their tweezer type structure, have been suggested as useful agents as molecular receptors, chiral solvating agents and inclusion complexes (Maitra et al., 1995).



1036

1037

1038

FIGURE 32. Proposed mechanism for epimerisation of a Tröger base by a) a proton catalysed ring opening or b) a retro-Diels-Alder mechanism, Révész et al., (2011).

1039

1040

1041

1042

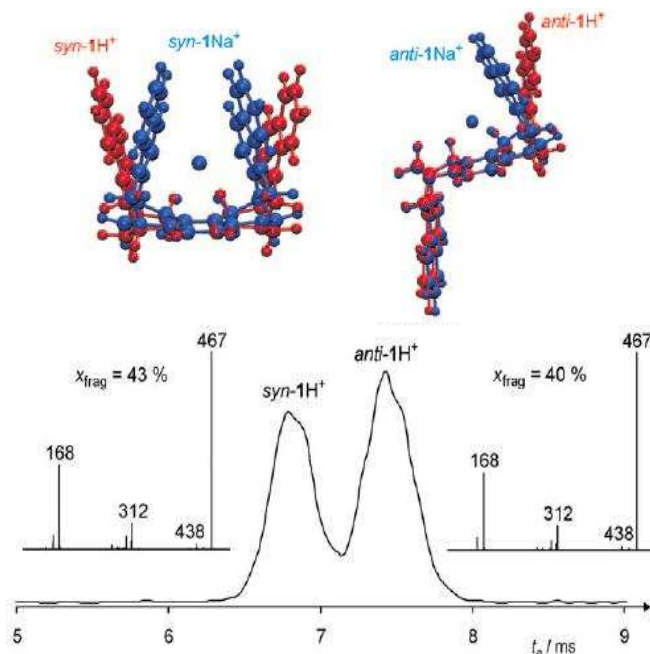
1043

1044

1045

The two structures were separated well in the gas-phase TWIMS stage (FIGURE 33) and activation of ions pre-TWIMS separation and post-TWIMS separation demonstrated that the anti-1H⁺ isomer is the most thermodynamically favoured by measuring the intensity of each parent ion. The preferred mechanism was also concluded to be the proton catalysed ring opening as demonstrated by the lack of epimerisation when a Na⁺ Tröger base was used as a surrogate proton-like participant in the reaction, thus eliminating the possibility of a retro-Diels-Alder mechanism.

1046



1047

1048 **FIGURE 33.** Ion mobility trace with associated mass spectra (shown inset) of the *anti*- and
 1049 *syn*- isomers. The computationally calculated structures are shown above, adapted from Révész et al.,
 1050 (2011).

1051 **B. Measurement of collision cross-section (CCS) for small molecules using DT-IMS-MS**

1052 The measurement of CCS in DT-IMS is simplified by the use of a static, uniform, electric field in which
 1053 ion motion takes place; the physical principles are established and mobility values can be used to
 1054 derive the collision cross-section. Knowing the length of the drift region and the time that ions take to
 1055 traverse it enables the ion's velocity to be determined:

1056

$$v = KE \rightarrow \frac{L}{t_d} = K \frac{V}{L} \rightarrow K = \frac{L^2}{Vt_d} \quad (9)$$

1058

1059

1060

1061 where v is the ion's velocity, K is the ion mobility constant, E is the electric field, L is the length of the
 1062 drift tube, t_d is the arrival time and V is the voltage across the drift region.

1063

1064 K should be corrected for temperature and pressure to obtain the reduced ion mobility, K_0 (corrected
 1065 to 273 K and 760 Torr):

1066

$$K_0 = K \left[\frac{273}{T} \right] \left[\frac{P}{760} \right] \quad (10)$$

1068

1069

1070

1071 The collision cross-section, Ω_T , can then be derived directly:

1072

$$\Omega_T = \left(\frac{3ze}{16N} \right) \left(\frac{2\pi}{\mu kT} \right)^{1/2} \left(\frac{1}{K} \right) \quad (11)$$

1074

1075

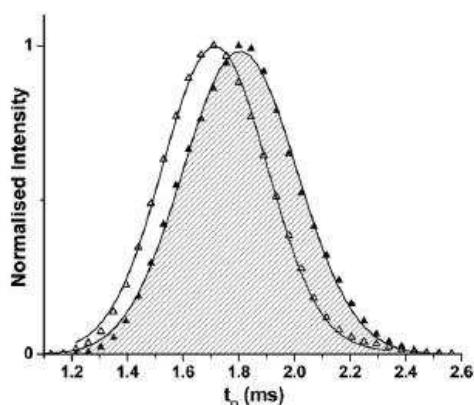
1076 where Ω is the collision cross-section, ze is the ionic charge, N is the background gas number density,
 1077 μ is the reduced mass of the ion-neutral pair, k is Boltzmann's constant, T is the gas temperature and

1078 K is the mobility constant.

1079 C. Calculation of collision cross-section (CCS) for small molecules using TWIMS

1080 The measurement of CCS in TWIMS is not typically directly derived from the mobility of an ion (Giles
1081 et al., 2010) as the motion of the analyte in the travelling wave regime is complicated and, to date, is
1082 not fully understood. The TWIMS system is, therefore, usually calibrated using ions that have
1083 previously been measured by employing DT-IMS. A typical calibration regime (Knapman et al., 2010)
1084 has been described based on the CCSs of oligo-glycine ions (available at
1085 <http://www.indiana.edu/~clemmer/>) which are currently accepted to be suitable as they are high
1086 mobility ions in the expected mobility range of small molecules, and have been measured previously
1087 using DT-IMS. Calibration with a static 4 V wave gave more drift time values over a narrower range of
1088 CCSs than a wave ramp, potentially resulting in greater resolving power. Although changes can be
1089 made to the buffer gas used in the measurement, the larger the buffer gas molecules, the larger the
1090 CCS and it was noted that the buffer gas radius used in theoretical calculations must be indicative of
1091 the buffer gas used in the original DT-IMS measurements (typically helium), even if the analysis of
1092 calibrants and analytes is carried out in a different buffer gas.

1093
1094 The experimental resolving power was reported under these conditions for the isomeric amino acids
1095 isoleucine and leucine (131 Da), calculated the CCS at 68.95 \AA^2 and 70.51 \AA^2 , respectively from the
1096 measured arrival time distributions (see Figure 34).
1097 .



1098
1099 **FIGURE 64.** Overlaid mobility chromatograms of L-Ile (open) and L-Leu (filled) acquired using a static
1100 4 V wave height. The ESI-TWIMS-MS experimental CCS values measured were 68.95 and 70.51 \AA^2 ,
1101 and the calculated CCS values were 70.81 and 72.03 \AA^2 , for L-Ile and L-Leu, respectively. Adapted
1102 from Knapman et al., (2010).

1103 To understand the differences between solution state and gas-phase measurements the theoretical
1104 collision cross-sections were calculated as a weighted average over multiple solution-phase rotameric
1105 states from a database of 5000 protein structures and compared to the experimentally measured gas-
1106 phase values (Table 4). Calculated CCS values for hydrophobic amino acids gave the best
1107 agreement with gas-phase TWIMS values, whilst more polar residues are experimentally found to be
1108 much smaller than calculated, mostly likely due to burying of polar and charged termini. The largest
1109 differences also appear to be correlated to the degrees of freedom in the amino acid side-chain.

1110
1111 **TABLE 4.** Comparison of measured and predicted CCS values for seven amino acids, adapted from
1112 Knapman et al., (2010).
1113

Amino acid	Mw (Da)	Rotamers	TWIMS experimental CCS (\AA^2)	CCS predicted from solution state (\AA^2)	Difference (\AA^2)	Notes
Pro	115.12	2	62.43	63.16	0.73	Hydrophobic
Val	117.15	3	64.81	64.82	0.01	Hydrophobic
Leu	131.12	4	70.51	72.03	1.52	Hydrophobic
Ile	131.12	4	68.95	70.81	1.86	Hydrophobic
Asp	133.11	5	62.93	69.81	6.88	Polar

Gln	146.15	5	62.85	75.08	12.23	Polar
Glu	147.13	7	63.35	76.69	13.34	Polar

1114
1115
1116
1117
1118

This demonstrates that IMS-MS can distinguish between subtle changes in shape e.g. differentiating Leu and Ile and also has the potential to reveal structural information about the important interactions present in the gas-phase such as the burial of the polar groups in the examples Gln and Glu.

1119 **D. Calculation of collision cross-section (CCS) for small molecules using overtone IMS-MS**

1120 Recently, overtone mobility spectrometry (Kurulugama et al., 2009; Valentine et al., 2009), where
1121 separation is achieved by applying time-dependent electric fields to sequential segments in a drift-
1122 tube thus eliminating ions that are not resonant with the applied field, has been used to demonstrate
1123 measurements of ion collision cross-sections:

1124

$$1126 \quad \Omega = \frac{(18\pi)^{1/2}}{16} \frac{ze}{(k_b T)^{1/2}} \left[\frac{1}{m_i} + \frac{1}{m_B} \right]^{1/2} \frac{E[\phi(h-1)+1]}{f(l_t + l_e)} \frac{760}{P} \frac{T}{273.2} \frac{1}{N} \quad (12)$$

1127
1128
1129
1130
1131
1132

where Ω is the collision cross-section, k_b is the Boltzmann constant, z is the ionic charge, e is the charge of an electron, N is the buffer gas density, T is the temperature of the buffer gas, P is the pressure of the buffer gas, E is the electric field, m_i and m_B are the masses of the ion and the buffer gas. The overtone IMS specific parameters include f which is the application frequency, h is the harmonic index, l_t is the ion transmission length and l_e is the ejection length.

1133
1134
1135
1136
1137
1138
1139
1140
1141

Reduced ion mobilities are reported to enable a comparison of DT-IMS-MS and overtone-IMS-MS measurements and are, in general, in good agreement. An especially interesting feature is the potential for overtone-IMS-MS to exclude different ion structures i.e. with different ion mobilities in the IMS stage. Typical IMS and TWIMS approaches are thought to measure an experimental average of all structures sampled within the IMS drift time, whereas overtone-IMS-MS appears to enable selection of particular structures over the IMS drift-time, potentially giving a better understanding of transitions on the IMS measurement timescale, in the order of a few milliseconds. Current measurements are limited for small molecules but development is ongoing.

1142 **E. Using theoretical calculations to understand ion mobility data**

1143 The assignment of structural information is typically made by comparing theoretical, calculated CCS
1144 values with experimentally determined CCS values by using the following procedures:

1145
1146
1147
1148
1149

1. generate list of conformers,
2. minimise structures to lowest energy structures,
3. calculation of theoretical CCS, and
4. comparison of theoretical CCS values with experimentally determined values.

1150
1151

1. Generate list of conformers

1152 Initially the molecule must be transformed from a flat 2D to a representative 3D structure at
1153 physiological pH taking into account tautomerism, likely protonation site(s), bond lengths etc. The
1154 accessible conformations can be explored for small molecules (Dear et al., 2010; Williams et al.,
1155 2009b) using methods including systematic search, molecular dynamics, random search and grid
1156 search tools but may be very computationally expensive if the number of rotatable bonds is high,
1157 requiring evaluation of thousands of potential structures for relatively simple structures.

1158
1159

2. Minimise structure to lowest energy structures

1160 Molecular dynamics approaches have been applied to small molecules with success and
1161 computationally are far less demanding than for large molecules (Baumketner et al., 2006; von
1162 Helden et al., 1995; Hoaglund-Hyzer et al., 1999; Jarrold, 2000; Kinnear et al., 2002). Methods have
1163 included force-field techniques including MMFF94 forcefield (Dear et al., 2010) and CHARM (Mao et
1164 al., 2001) but quantum mechanical methods e.g., density functional theory (DFT) may also be feasible
1165 for understanding small molecule structures. Indeed DFT has almost become the 'norm' for

1166 calculating ion structures (Holmes et al., 1985), as it is more accurate than semi-empirical methods .
1167 Recent work (Alex et al., 2009; Wright et al., 2010) has highlighted the potential for DFT to
1168 understand electron density in bond formation/cleavage and the effect of protonation on bond lengths,
1169 which makes DFT a potentially powerful tool in modelling ion structures in IMS-MS. Indeed the
1170 information obtained from DFT calculations may contribute to a better understanding of the ion
1171 structure for both the IMS separation and any tandem MS results.

1172 **3. Calculation of theoretical CCS**

1173 The main calculation protocols for obtaining theoretical CCS values in IMS include projection
1174 approximation (PA), trajectory method (TJ) and exact hard sphere scattering (EHSS). Whilst there has
1175 been some debate about which type of modelling is most appropriate, it is generally recommended to
1176 use the projection approximation (PA) method for small molecules of 20-100 atoms, for example
1177 using the Sigma software package or MOBCAL software. However, PA typically underestimates
1178 collision cross-sections for polyatomic species, especially for different surfaces including concave
1179 structures, by up to 20% (Shvartsburg and Jarrold, 1996), so is not typically recommended for larger
1180 molecular weight structures.

1181 TJ typically works well for any size system, but calculations are computationally expensive. Exact
1182 Hard Sphere Scattering (EHSS) typically fails with small molecules because the ion-buffer gas
1183 interaction becomes important compared to the geometry of the ion and careful calibration of the
1184 relevant atomic radii is essential (Shvartsburg and Jarrold, 1996). EHSS and TJ appear to provide
1185 better agreement for larger molecular weight ions as the parameterisation of EHSS is based on
1186 fullerenes and other large molecular weight ions.

1187 There have been attempts to improve modelling, for large molecules (Shvartsburg et al., 2007) and
1188 small molecules (Knapman et al., 2010; Siu et al., 2010), by construction of new parameter basis sets
1189 with values for the carbon, oxygen, helium and nitrogen interaction radius calculated from suitable
1190 representative molecules. Further development of modelling and prediction techniques (Fernandez-
1191 Lima et al., 2009) and improvement in parameter basis sets may well provide closer agreement
1192 between calculated and measured CCSs. Recent improvements to a nitrogen based trajectory
1193 method (Campuzano et al. 2011) may help understand data generated in $N_{2(g)}$ (as the less polarizable
1194 $He_{(g)}$ is typically used) and create better calibrations for collision cross sections (especially useful in
1195 TWIMS where $N_{2(g)}$ is the typical drift gas). The set of collision cross sections for pharmaceutically
1196 relevant 'small molecule' compounds appears self consistent ($R^2 = 0.9949$) and covers a useful range
1197 of 124.5 to 254.3 \AA^2 for nitrogen gas and a range of 63.0 to 178.8 \AA^2 for helium gas.

1200 **4. Comparison of calculated CCS values with experimentally determined values**

1201 Typically validation is best achieved using known standards within experimental sets, either for
1202 relative ranking of results or to increase confidence in measurements. Structure co-ordination sets are
1203 widely available for some species e.g. at the RCSB Protein Data Bank and have been data based by
1204 Clemmer (available at
1205 [http://www.indiana.edu/~eclemmer/Research/cross%20section%20database/Proteins/protein_cs.ht](http://www.indiana.edu/~eclemmer/Research/cross%20section%20database/Proteins/protein_cs.htm)
1206 [m](http://www.indiana.edu/~eclemmer/Research/cross%20section%20database/Proteins/protein_cs.htm)). However, it should be noted that the co-ordination structures from different sources may not agree
1207 as NMR structures are often subject to solvent effects, x-ray structures subject to crystal lattice effects
1208 and measurements by ion mobility may be subject to gas-phase neutral contamination, ionisation and
1209 solvent effects. Some publications describe the calculation of theoretical collision-cross sections using
1210 datasets obtained from NMR and x-ray files (e.g. PDB files) as input without subsequent energy
1211 minimisation in the gas-phase which could result in erroneous estimates of CCS and further
1212 assignment; in such a case a better understanding via structure/energy minimisation may be
1213 important.

1215 **VI. PREDICTION OF ION MOBILITY CONSTANTS**

1216 Whilst many approaches to IMS explicitly use or attempt to derive information on the 3D structure of
1217 the ion another approach is to use molecular descriptors to adequately describe an ion and predict
1218 the reduced mobility without any requirement to carry out computationally expensive geometry
1219 optimisation. A quantitative structure property relationship (QSPR) methodology using five
1220 descriptors for a training set of 70 organic compounds and excluding three outliers gave a multi-linear
1221 regression (MLR) of $R^2 = 0.98$ and $s = 0.047$; the test set of seven compounds gave $s = 0.047$
1222 (Wessel and Jurs, 1994). Later, using six molecular descriptors on a training set of 135 compounds
1223 and testing the model with 18 compounds gave an RMS error of 0.038 (Wessel et al., 1996). A more
1224

1225 diverse set of 182 compounds and modification of two of the descriptors correlated with an $R^2 = 0.80$
1226 (Agbonkonkon et al., 2004). A subset of 159 of that data set was used to develop linear and non-
1227 linear models using MLR and progression pursuit regression to achieve R^2 values of 0.908 and 0.938
1228 and $s = 0.066$ and 0.055 , respectively (Liu et al., 2007a). The recent formulation of a linear equation
1229 for ion mobility in a series of polar aliphatic organic compounds resulted in ion mobility predictions that
1230 were typically >99% accurate (Hariharan et al., 2010).

1231
1232 These molecular descriptor approaches are now widely used in predicting peptide IMS-MS drift times
1233 (Wang et al., 2010) to improve confidence in peptide identification. The same approach to prediction
1234 of 'small molecule' IMS-MS drift times could well help refine models of drift time prediction and better
1235 understand important interactions affecting drift time and thus gas-phase structures, however this is
1236 currently not well understood.

1237 VII. FUTURE DEVELOPMENTS

1238 The adoption of IMS-MS both for small molecule as well as large molecule applications is likely to
1239 continue strongly, assisted by rapid developments in IMS design that marries the two stages of IMS
1240 and MS and mitigates the challenges of ion efficiency and resolution that has hindered their
1241 combination.

1242
1243 The resistive glass-IMS design recently invented to replace the traditional stacked-ring ion guides
1244 enables easier construction (Kwasnik and Fernández, 2010) and designs include a segmented rf
1245 quadrupole in the vacuum interface that improve sensitivity by over 2 order of magnitude (Kaplan et
1246 al., 2010). The inverse ion mobility spectrometry technique that applies an inverted pulse to the
1247 shutter grid appears to increase resolution by 30-60% presumably by creating a gap in the charge
1248 cloud and thus reducing space-charging effects (Tabrizchi and Jazan, 2010).

1249
1250 A further hyphenation of a photoelectron spectrometer to a IMS-TOFMS shows promise as a
1251 complementary method to obtain further information on the structures of gas-phase ions by obtaining
1252 photoelectron spectra at three different detachment laser wavelengths (Vonderach et al., 2011), and
1253 also hints at the possibilities for further information-rich data to be acquired and combined with IMS-
1254 MS by further hyphenation.

1255
1256 The adoption of IMS in hyphenated IMS-MS systems is continuing with important developments, for
1257 example, Agilent previously announced collaborations with Owlstone Nanotechnologies for an IMS-
1258 MS system and Bruker have investigated new modes of IMS (Baykut et al., 2009). There have been
1259 long-term research investments demonstrated in the launch of the second generation Waters Synapt
1260 G2 IMS-MS with improved resolution and ion transmission and with the AB Sciex SelexION
1261 technology that is available for the AB Sciex Triple Quad 5500 and QTRAP 5500 Systems including
1262 selection of gas-phase dopants which can improve IMS separation and rapid 25 ms cycle time per
1263 MRM which matches cycle times with multi-component analysis and UHPLC time scales.

1264

1265 VIII. CONCLUSIONS

1266 Whilst IMS is a ubiquitous technique in airports as well as military and forensic applications, it is still
1267 the case that using IMS-MS for measuring structural information and for separations in 'small
1268 molecule' applications there are subtle differences that can significantly affect the mobility and there is
1269 much more to be understood about how to measure the structures of gas-phase ions reliably, the
1270 nature of the fundamental intra-molecular interactions that define the structures and what the effect of
1271 ion-neutral interactions are on ion mobility.

1272
1273 Many chemical classes have been investigated using IMS and IMS-MS and some of the main
1274 publications are listed in Table 5 to direct the reader to more detail on those classes.

1275 **TABLE 5.** Applications of IMS-MS and IMS to 'small molecule' classes.

1276

Class	Year
Hydrocarbons (Creaser et al., 2004)	1973
Halogenated benzenes and nitro benzenes (o-, m-substituted) (Karpas et al., 1988)	1973
Dihalogenated benzenes (o-, m-substituted) (Karpas et al., 1988)	1974

Benzoic and isophthalic and phthalic acids (Karpas et al., 1988)	1975
Some sec-butylchlorodiphenyl oxides (Karpas et al., 1988)	1976
o- and p- substituted chlorodiphenyl oxides (Karpas et al., 1988)	1976
Ethyl butyl esters of maleic and fumaric (Karpas et al., 1988)	1982
Succinic acids (Karpas et al., 1988)	1982
Isomeric ketones 2-octanone vs. 4,4-dimethyl-3-hexanone (Karpas et al., 1988)	1986
Isomeric alcohols 1-octanol vs. 2-octanol (Karpas et al., 1988)	1986
Substituted electrophilic olefins, keto enol isomers, 2 keto and 2 enol (Karpas et al., 1988)	1988
Amides and amines (Karpas et al., 1988) (Karpas et al., 1994)	1989 & 1994
Anilines (Karpas et al., 1990b)	1990
Simple monocyclic and dicyclic compounds (Karpas et al., 1990a)	1990
Aminoazoles (Karpas and Tironi, 1991)	1991
Ketones (Karpas, 1991)	1991
Aminoalcohols (Karpas, 1992)	1991
Benzodiazepines, amphetamines and opiates (Karpas et al., 1988)	2001 & 2002
Amino acids (Asbury & Hill, 2000b)	2001
Amphetamines (Matz and Hill, 2002)	2002

1277

1278

1279

1280

1281

1282

Standardized calibration and measurement methods (Fernández-Maestre et al., 2010b), easily implemented and accurate predictive models and interpretation of results are still being developed but show great promise. The interchange between academia, vendors and industry is ensuring more options are available to potential users of IMS-MS. A range of current commercial manufacturers and IMS-MS types are listed in Table 6 for reference.

1283

TABLE 6. Commercially available IMS systems, or accessories able to interface to MS systems.

IMS-MS manufacturer	Type
Excellims IMS-MS	DT-IMS
Tofwerk IMS-MS	DT-IMS
Waters Synapt IMS-MS	TWIMS
Thermo FAIMS cylindrical electrode	FAIMS
Owlstone Nanotech	FAIMS
AB Sciex SelexION parallel plate	DMS
Sionex microDMx	DMS

1284

1285

1286

1287

1288

1289

1290

1291

1292

1293

1294

1295

Over the last decade there have been many novel applications and developments in IMS-MS involving new methods to generate ions, accumulate and focus ions, select ions preferentially, measure and process the multiplexed information and they have been used to solve problems ranging from hydration/desolvation in 'small' organic molecules to understanding the fundamental interactions in the building blocks of life, amino acids. IMS-MS is a novel method that can separate ions and use information on their mobility to assign structure on an unparalleled rapid timeframe and at high levels of sensitivity. In combination with a range of analytical equipment including ionisation sources, separation devices, solution chemistry and gas-phase chemistry; the use of IMS-MS offers a versatile and powerful approach to unique insights into complex mixtures and hitherto ambiguous structures.

1296

REFERENCES

1297

1298

1299

Agbonkonkon N, Tolley HD, Asplund MC, Lee ED, Lee ML. 2004. Prediction of gas-phase reduced ion mobility constants (K0). *Anal Chem* 76:5223-5229.

1300

1301

Aksenov AA, Kapron JT. 2010. Behaviour of tetraalkylammonium ions in high-field asymmetric waveform ion mobility spectrometry. *Rapid Commun Mass Spectrom* 24:1392-1396.

1302

1303

Albritton DL, Miller TM, Martin DW, McDaniel EW. 1968. Mobilities of mass-identified H₃⁺ and H⁺ ions in hydrogen. *Phys Rev* 171:94.

1304

1305

Alex A, Harvey S, Parsons T, Pullen FS, Wright P, Riley, JA. (2009). Can density functional theory (DFT) be used as an aid to a deeper understanding of tandem mass spectrometric fragmentation pathways?. *Rapid Commun Mass Spectrom*, 23: 2619–2627

1306

- 1307 Allen FH, Harris SE, Taylor R. 1996. Comparison of conformer distributions in the crystalline state
1308 with conformational energies calculated by *ab initio* techniques. *J Comput-Aid Mol Des*
1309 10:247-254.
- 1310 Alonso R, Rodríguez-Estévez V, Domínguez-Vidal A, Ayora-Cañada MJ, Arce L, Valcárcel M. 2008.
1311 Ion mobility spectrometry of volatile compounds from iberian pig fat for fast feeding regime
1312 authentication. *Talanta* 76:591-596.
- 1313 Project Summary. Recovery.gov.
1314 <http://www.recovery.gov/Transparency/RecipientReportedData/pages/RecipientProjectSummary508.aspx?AwardIDSUR=93260&qtr=2010Q3>.
1315
- 1316 Arthur KE, Wolff J, Carrier DJ. 2004. Analysis of betamethasone, dexamethasone and related
1317 compounds by liquid chromatography/electrospray mass spectrometry. *Rapid Commun Mass*
1318 *Spectrom* 18: 678-684
- 1319 Asbury GR, Hill HH. 2000a. Evaluation of ultrahigh resolution ion mobility spectrometry as an
1320 analytical separation device in chromatographic terms. *J. Micro Sep* 12:172-178.
- 1321 Asbury GR, Hill HH. 2000b. Separation of amino acids by ion mobility spectrometry. *J Chromatog A*
1322 902:433-437.
- 1323 Asbury GR, Hill HH. 2000c. Using Different Drift Gases To Change Separation Factors (α) in Ion
1324 Mobility Spectrometry. *Anal. Chem.*72: 580-584
- 1325 Aston FW. 1919. A positive ray spectrograph. *Philos. Mag.*, 38: 707-715.
- 1326 Baim MA, Hill HH. 1982. Tunable selective detection for capillary gas chromatography by ion mobility
1327 monitoring. *Anal Chem* 54:38-43.
- 1328 Baker ES, Bushnell JE, Wecksler SR, Lim MD, Manard MJ, Dupuis NF, Ford PC, Bowers MT. 2005.
1329 Probing shapes of bichromophoric metal-organic complexes using ion mobility mass
1330 spectrometry. *J Am Chem Soc* 127:18222-18228.
- 1331 Barnes WS, Martin DW, McDaniel EW. 1961. Mass spectrographic identification of the ion observed
1332 in hydrogen mobility experiments. *Phys. Rev Lett* 6:110.
- 1333 Bastug T, Kuyucak S. 2003. Role of the dielectric constants of membrane proteins and channel water
1334 in ion permeation. *Biophys J* 84:2871-2882.
- 1335 Baumketner A, Bernstein SL, Wyttenbach T, Lazo ND, Teplow DB, Bowers MT, Shea J-E. 2006.
1336 Structure of the 21-30 fragment of amyloid β -protein. *Protein Sci* 15:1239-1247.
- 1337 Baykut G, von Halem O, Raether O. 2009. Applying a Dynamic Method to the Measurement of Ion
1338 Mobility. *J Am Soc Mass Spectrom*, 20: 2070-2081
- 1339 Beegle LW, Kanik I, Matz L, Hill HH. 2001. Electrospray ionization high-resolution ion mobility
1340 spectrometry for the detection of organic compounds, 1. amino acids. *Anal Chem* 73:3028-
1341 3034.
- 1342 Belov ME, Clowers BH, Prior DC, Danielson III WF, Liyu AV, Petritis BO, Smith RD. 2008.
1343 Dynamically multiplexed ion mobility time-of-flight mass spectrometry. *Anal Chem* 80:5873-
1344 5883.
- 1345 Bluhm BK, Gillig KJ, Russell DH. 2000. Development of a fourier-transform ion cyclotron resonance
1346 mass spectrometer-ion mobility spectrometer. *Rev Sci Instrum* 71:4078.
- 1347 Bohrer BC, Merenbloom SI, Koeniger SL, Hilderbrand AE, Clemmer DE. 2008. Biomolecule analysis
1348 by ion mobility spectrometry. *Ann Rev Anal Chem* 1:293-327.
- 1349 Budimir N, Weston DJ, Creaser CS. 2007. Analysis of pharmaceutical formulations using atmospheric
1350 pressure ion mobility spectrometry combined with liquid chromatography and nano-
1351 electrospray ionisation. *Analyst* 132:34.
- 1352 Buryakov IA, Krylov EV, Nazarov EG, Rasulev UK. 1993. A new method of separation of multi-atomic
1353 ions by mobility at atmospheric pressure using a high-frequency amplitude-asymmetric strong
1354 electric field. *Int J Mass Spectrom.* 128:143-148
- 1355 Canterbury JD, Yi X, Hoopmann MR, MacCoss MJ. 2008. Assessing the dynamic range and peak
1356 capacity of nanoflow lc-faims-ms on an ion trap mass spectrometer for proteomics. *Anal*
1357 *Chem* 80:6888-6897.
- 1358 Campuzano I, Bush MF, Robinson CV, Beaumont C, Richardson K, Kim H, Kim HI. 2012. Structural
1359 Characterization of Drug-like Compounds by Ion Mobility Mass Spectrometry: Comparison of
1360 Theoretical and Experimentally Derived Nitrogen Collision Cross Sections. *Anal Chem* 84
1361 (2):1026-1033.
- 1362 Champarnaud E, Laures AM-F, Borman PJ, Chatfield MJ, Kapron JT, Harrison M, Wolff J-C. 2009.
1363 Trace level impurity method development with high-field asymmetric waveform ion mobility
1364 spectrometry: systematic study of factors affecting the performance. *Rapid Commun Mass*
1365 *Spectrom* 23:181-193.

- 1366 Clemmer DE. 1997. Injected-ion mobility analysis of biomolecules.
1367 <http://www.indiana.edu/~clemmer/Publications/pub%20042.pdf>.
- 1368 Clowers BH, Ibrahim YM, Prior DC, Danielson WF, Belov ME, Smith RD. 2008. Enhanced ion
1369 utilization efficiency using an electrodynamic ion funnel trap as an injection mechanism for ion
1370 mobility spectrometry. *Anal. Chem* 80:612-623.
- 1371 Clowers BH, Hill HH. 2006. Influence of cation adduction on the separation characteristics of flavonoid
1372 diglycoside isomers using dual gate-ion mobility-quadrupole ion trap mass spectrometry. *J*
1373 *Mass Spectrom* 41:339-351.
- 1374 Clowers BH, Siems WF, Hill HH, Massick SM. 2006. Hadamard transform ion mobility spectrometry.
1375 *Anal Chem* 78:44-51.
- 1376 Collins DC, Lee ML. 2001. Electrospray ionization gas-phase electrophoresis under ambient
1377 conditions and it's potential or high-speed separations. *Fresenius' J Anal Chem* 369:225-233.
- 1378 Covey T, Douglas DJ. 1993. Collision cross sections for protein ions. *J. Am. Soc. Mass Spectrom*.4:
1379 616-623
- 1380
- 1381 Coy SL, Krylov EV, Schneider BB, Covey TR, Brenner DJ, Tyburski JB, Patterson AD, Krausz KW,
1382 Fornace AJ, Nazarov EG.2010.Detection of Radiation-Exposure Biomarkers by Differential
1383 Mobility Prefiltered Mass Spectrometry (DMS-MS). *Int. J. Mass Spectrom.* 291: 108-117
- 1384 Creaser CS, Benyazzar M, Griffiths JR, Stygall JW. 2000. A tandem ion trap/ion mobility spectrometer.
1385 *Anal Chem* 72:2724-2729.
- 1386 Creaser CS, Griffiths JR, Bramwell CJ, Noreen S, Hill CA, Thomas CLP. 2004. Ion mobility
1387 spectrometry: a review. part 1. structural analysis by mobility measurement. *Analyst* 129:984.
- 1388 Cui M, Ding L, Mester Z. 2003. Separation of cisplatin and its hydrolysis products using electrospray
1389 ionization high-field asymmetric waveform ion mobility spectrometry coupled with ion trap
1390 mass spectrometry. *Anal Chem* 75:5847-5853.
- 1391 Cuyckens F, Wassvik C, Mortishire - Smith RJ, Tresadern G, Campuzano I, Claereboudt J. 2011.
1392 Product ion mobility as a promising tool for assignment of positional isomers of drug
1393 metabolites. *Rapid Commun Mass Spectrom.* 25:3497-3503
- 1394 D'Agostino PA, Chenier CL. 2010. Desorption electrospray ionization mass spectrometric analysis of
1395 organophosphorus chemical warfare agents using ion mobility and tandem mass
1396 spectrometry. *Rapid Commun Mass Spectrom* 24:1617-1624.
- 1397 Dear GJ, Munoz-Muriedas J, Beaumont C, Roberts A, Kirk J, Williams JP, Campuzano I. 2010. Sites
1398 of metabolic substitution: investigating metabolite structures utilising ion mobility and
1399 molecular modelling. *Rapid Commun Mass Spectrom* 24:3157-3162.
- 1400 de la Mora JF, Ude S, Thomson BA. 2006. The potential of differential mobility analysis coupled to
1401 MS for the study of very large singly and multiply charged proteins and protein complexes in
1402 the gas phase. *Biotechnol. J.* 1: 988-997
- 1403 Douglas DH. 1998. Applications of Collision Dynamics in Quadrupole Mass Spectrometry. *J Am Soc*
1404 *Mass Spectrom.* 9: 101-113
- 1405 Dussy FE, Berchtold C, Briellmann TA, Lang C, Steiger R, Bovens M. 2008. Validation of an ion
1406 mobility spectrometry (ims) method for the detection of heroin and cocaine on incriminated
1407 material. *Forensic Sci Int* 177:105-111.
- 1408 Dwivedi P, Bendiak B, Clowers BH, Hill HH. 2007. Rapid resolution of carbohydrate isomers by
1409 electrospray ionization ambient pressure ion mobility spectrometry-time-of-flight mass
1410 spectrometry (esi-apims-tofms). *J Am Soc Mass Spectrom* 18:1163-1175.
- 1411 Dwivedi P, Schultz AJ, Jr HHH. 2010. Metabolic profiling of human blood by high-resolution ion
1412 mobility mass spectrometry (im-ms). *Int J Mass Spectrom* 298:78-90.
- 1413 Dwivedi P, Wu C, Matz LM, Clowers BH, Siems WF, Hill HH. 2006. Gas-phase chiral separations by
1414 ion mobility spectrometry. *Anal Chem* 78:8200-8206.
- 1415 Eatherton RL, Morrissey MA, Siems WF, Hill HH. 1986. Ion mobility detection after supercritical fluid
1416 chromatography. *J High Res Chromatogr* 9:154-160.
- 1417 Eiceman GA, Karpas Z. 2004. Ion mobility spectrometry. 2nd edition. Boca Raton, FL, USA: CRC
1418 Press
- 1419 Eiceman GA, Yuan-Feng W, Garcia-Gonzalez L, Harden CS, Shoff DB. 1995. Enhanced selectivity in
1420 ion mobility spectrometry analysis of complex mixtures by alternate reagent gas chemistry.
1421 *Anal Chim Acta* 306:21-33.
- 1422 Eiceman GA, Krylov EV, Krylova NS, Nazarov EG, Miller RA. 2004. Separation of Ions from
1423 Explosives in Differential Mobility Spectrometry by Vapor-Modified Drift Gas. *Anal. Chem.* 76:
1424 4937-4944

- 1425 Enders JR, Mclean JA. 2009. Chiral and structural analysis of biomolecules using mass spectrometry
1426 and ion mobility - mass spectrometry. *Chirality* 21:E253-E264.
- 1427 Fenn LS, McLean JA. 2008. Enhanced carbohydrate structural selectivity in ion mobility-mass
1428 spectrometry analyses by boronic acid derivatization. *Chem. Comm.* 13:5505-5507
- 1429 Fernandez-Lima FA, Wei H, Gao YQ, Russell DH. 2009. On the structure elucidation using ion
1430 mobility spectrometry and molecular dynamics. *J Phys Chem A* 113:8221-8234.
- 1431 Fernández-Maestre R, Wu C, Hill Jr. HH. 2010. Using a buffer gas modifier to change separation
1432 selectivity in ion mobility spectrometry *Int J Mass Spectrom* 298:2-9.
- 1433 Fernandez-Maestre R, Harden CS, Ewing RG, Crawford CL, Hill Jr. HH. 2010. Chemical standards in
1434 ion mobility spectrometry. *The Analyst*.135:1433-1442
- 1435 Foloppe N, Chen I-J. 2009. Conformational sampling and energetics of drug-like molecules. *Curr.*
1436 *Med Chem* 16:3381-3413.
- 1437 Gehrke CW. 2001. *Chromatography: a century of discovery 1900-2000: the bridge to the*
1438 *sciences/technology*. Boca Raton, FL, USA: Elsevier.
- 1439 Gerlich D. 1992 In: *State-Selected and State-to-State Ion-Molecule Reaction Dynamics*. Part 1. Ng
1440 CY, Baer M, editors. LXXXII. John Wiley; New York: pp. 1-176
- 1441 Giles K, Wildgoose JL, Langridge DJ, Campuzano I. 2010. A method for direct measurement of ion
1442 mobilities using a travelling wave ion guide. *Int J Mass Spectrom* 298:10-16
- 1443 Giles K, Williams JP, Campuzano I. 2011. Enhancements in travelling wave ion mobility resolution.
1444 *Rapid Comm Mass Spectrom* 25:1559-1566.
- 1445 Gorshkov MP. 1982. Inventor's certificate USSR no. 966583 Byull Izobret 38.
- 1446 Griffin GW, Dzidic I, Carroll DI, Stillwell RN, Horning EC. 1973. Ion mass assignments based on
1447 mobility measurements. validity of plasma chromatographic mass mobility correlations. *Anal*
1448 *Chem* 45:1204-1209.
- 1449 Guevremont R, Purves RW. 1999. Atmospheric pressure ion focusing in a high-field asymmetric
1450 waveform ion mobility spectrometer. *Rev. Sci. Instrum.* 70: 1370-1384
- 1451 Guo Y, Wang J, Javahery G, Thomson BA, Siu KWM. 2004. Ion Mobility Spectrometer with Radial
1452 Collisional Focusing. *Anal. Chem.* 77:266-275
- 1453 Guo Y, Srinivasan S, Gaiki S. 2009. Evaluation of the peak capacity of various rp-columns for small
1454 molecule compounds in gradient elution. *Chromatographia* 70:1045-1054.
- 1455 Hariharan CB, Baumbach JI, Vautz W. 2010. Linearized equations for the reduced ion mobilities of
1456 polar aliphatic organic compounds. *Anal Chem* 82:427-431.
- 1457 Harry EL, Reynolds JC, Bristow AWT, Wilson ID, Creaser CS. 2009. Direct analysis of pharmaceutical
1458 formulations from non-bonded reversed-phase thin-layer chromatography plates by
1459 desorption electrospray ionisation ion mobility mass spectrometry. *Rapid Commun Mass*
1460 *Spectrom* 23:2597-2604.
- 1461 Harry EL, Bristow AWT, Wilson ID, Creaser CS. 2011. Real-time reaction monitoring using ion
1462 mobility-mass spectrometry. *Analyst* 136:1728.
- 1463 Harvey SR, MacPhee CE, Barran PE, 2011. Ion mobility mass spectrometry for peptide analysis,
1464 *Methods*, 54, 4: 454-461
- 1465 Hatsis P, Brockman AH, Wu J-T. 2007. Evaluation of high-field asymmetric waveform ion mobility
1466 spectrometry coupled to nanoelectrospray ionization for bioanalysis in drug discovery. *Rapid*
1467 *Commun Mass Spectrom* 21:2295-2300.
- 1468 Heck AJR, van den Heuvel RHH. 2004. Investigation of intact protein complexes by mass
1469 spectrometry. *Mass Spectrom Rev* 23:368-389.
- 1470 von Helden G, Wyttenbach T, Bowers MT. 1995. Conformation of macromolecules in the gas phase:
1471 use of matrix-assisted laser desorption methods in ion chromatography. *Science* 267:1483-
1472 1485.
- 1473 Henderson SC, Valentine SJ, Counterman AE, Clemmer DE. 1999. Esi/ion trap/ion mobility/time-of-
1474 flight mass spectrometry for rapid and sensitive analysis of biomolecular mixtures. *Anal Chem*
1475 71:291-301.
- 1476 Hill CA, Thomas CLP. 2003. A pulsed corona discharge switchable high resolution ion mobility
1477 spectrometer-mass spectrometer. *Analyst* 128:55-60.
- 1478 Hoaglund-Hyzer CS, Counterman AE, Clemmer DE. 1999. Anhydrous protein ions. *Chem Rev*
1479 99:3037-3080.
- 1480 Hogan CJ, Ruotolo BT, Robinson CV, Fernandez de la Mora J. 2011. Tandem Differential Mobility
1481 Analysis-Mass Spectrometry Reveals Partial Gas-Phase Collapse of the GroEL Complex.
1482 *Phys. Chem. B*.115:3614-3621

- 1483 Hogg AM, Kebarle P. 1965 Mass-Spectrometric Study of Ions at Near-Atmospheric Pressure. II.
1484 Ammonium Ions Produced by the Alpha Radiolysis of Ammonia and Their Solvation in the
1485 Gas Phase by Ammonia and Water Molecules. *J. Chem. Phys.* 43:449-457
1486 Holmes JL. 2006. Assigning structures to ions in the gas phase. New York: CRC Press.
1487 Homans SW. 2007. Water, water everywhere--except where it matters? *Drug Discov Today* 12:534-
1488 539.
1489 Howdle MD, Eckers C, Laures AM-F, Creaser CS. 2009. The use of shift reagents in ion mobility-
1490 mass spectrometry: studies on the complexation of an active pharmaceutical ingredient with
1491 polyethylene glycol excipients. *J Am Soc Mass Spectrom* 20:1-9.
1492 Howdle MD, Eckers C, Laures AM-F, Creaser CS. 2010. The effect of drift gas on the separation of
1493 active pharmaceutical ingredients and impurities by ion mobility-mass spectrometry. *Int J*
1494 *Mass Spectrom* 298:72-77.
1495 Huang MX, Markides KE, Lee ML. 1991. Evaluation of an ion mobility detector for supercritical fluid
1496 chromatography with solvent-modified carbon dioxide mobile phases. *Chromatographia*
1497 31:163-167.
1498 Ibrahim YM, Meot-Ner M, Alshraeh EH, El-Shall MS, Scheiner S. 2005. Stepwise hydration of ionized
1499 aromatics. energies, structures of the hydrated benzene cation, and the mechanism of
1500 deprotonation reactions. *J Am Chem Soc* 127:7053-7064.
1501 Jackson SN, Ugarov M, Egan T, Post JD, Langlais D, Schultz JA, Woods AS. 2007. Maldi-ion
1502 mobility-tofms imaging of lipids in rat brain tissue. *J Mass Spectrom* 42:1093-1098.
1503 Jafari MT, Khayamian T, Shaer V, Zarei N. 2007. Determination of veterinary drug residues in chicken
1504 meat using corona discharge ion mobility spectrometry. *Anal Chim Acta* 581:147-153.
1505 Jafari MT. 2006. Determination and identification of malathion, ethion and dichlorovos using ion
1506 mobility spectrometry. *Talanta* 69:1054-1058.
1507 Javahery G, Thomson B. 1997. A segmented radiofrequency-only quadrupole collision cell for
1508 measurements of ion collision cross section on a triple quadrupole mass spectrometer. *J. Am.*
1509 *Soc. Mass Spectrom.* 8:697-702
1510 Jarrold MF. 2000. Peptides and proteins in the vapor phase. *Annu Rev Phys Chem* 51:179-207.
1511 Jurneczko E, Barran PE. 2011. How useful is ion mobility mass spectrometry for structural biology?
1512 the relationship between protein crystal structures and their collision cross sections in the gas
1513 phase. *Analyst* 136:20.
1514 Kanu AB, Dwivedi P, Tam M, Matz L, Hill HH. 2008. Ion mobility-mass spectrometry. *J. Mass*
1515 *Spectrom* 43:1-22.
1516 Kaplan K, Graf S, Tanner C, Gonin M, Fuhrer K, Knochenmuss R, Dwivedi P, Hill HH. 2010. Resistive
1517 glass im-tofms. *Anal Chem* 82:9336-9343.
1518 Karasek FW, Hill HH, Kim SH. 1976. Plasma chromatography of heroin and cocaine with mass-
1519 identified mobility spectra. *J Chromatogr* 117:327-336.
1520 Karimi A, Alizadeh N. 2009. Rapid analysis of captopril in human plasma and pharmaceutical
1521 preparations by headspace solid phase microextraction based on polypyrrole film coupled to
1522 ion mobility spectrometry. *Talanta* 79:479-485.
1523 Karpas Z, Bell SE, Wang Y-F, Walsh M, Eiceman GA. 1994. The structure of protonated diamines
1524 and polyamines. *Struct Chem* 5:135-140.
1525 Karpas Z. 1991. The structure and mobility in air of protonated ketones. *Int J Mass Spectrom*
1526 107:435-440.
1527 Karpas Z. 1992. The mobility of protonated aminoalcohols: evidence for proton-induced cyclization.
1528 *Struct Chem* 3:139-141.
1529 Karpas Z, Berant Z, Shahal O. 1990. The effects of saturation and substitution on the mobility of
1530 protonated cyclic compounds. *Int J Mass Spectrom Ion Proc* 96:291-297.
1531 Karpas Z, Berant Z, Stimac RM. 1990. An ion mobility spectrometry/mass spectrometry (ims/ms)
1532 study of the site of protonation in anilines. *Struct Chem* 1:201-204.
1533 Karpas Z, Stimac RM, Rappoport Z. 1988. Differentiating between large isomers and derivation of
1534 structural information by ion mobility spectrometry / mass spectrometry techniques. *Int J Mass*
1535 *Spectrom Ion Proc* 83:163-175.
1536 Karpas Z, Tironi C. 1991. The mobility and ion structure of protonated aminoazoles. *Struct Chem*
1537 2:655-659.
1538 Kebarle P, Hogg AM. 1965. Mass-Spectrometric Study of Ions at Near Atmospheric Pressures. I. The
1539 Ionic Polymerization of Ethylene. *The Journal of Chemical Physics.* 42: 668-675
1540 Keller T, Keller A, Tutsch-Bauer E, Monticelli F. 2006. Application of ion mobility spectrometry in
1541 cases of forensic interest. *Forensic Sci Int* 161:130-140.

- 1542 Kemper PR, Dupuis NF, Bowers MT. 2009. A new, higher resolution, ion mobility mass spectrometer.
1543 Int J Mass Spectrom 287:46-57.
- 1544 Kinnear BS, Hartings MR, Jarrold MF. 2002. The energy landscape of unsolvated peptides: helix
1545 formation and cold denaturation in ac-a4g7a4 + h+. J Am Chem Soc 124:4422-4431.
- 1546 Knapman TW, Berryman JT, Campuzano I, Harris SA, Ashcroft AE. 2010. Considerations in
1547 experimental and theoretical collision cross-section measurements of small molecules using
1548 travelling wave ion mobility spectrometry-mass spectrometry. Int J Mass Spectrom 298: 17-23.
- 1549 Knutson E, Whitby K. 1975. Aerosol classification by electric mobility: Apparatus, theory, and
1550 applications. J. Aerosol Sci. 6 (6): 443-451 Koeniger SL, Merenbloom SI, Clemmer DE. 2006.
1551 Evidence for many resolvable structures within conformation types of electrosprayed ubiquitin
1552 ions. J Phys Chem B 110:7017-7021.
- 1553 Kolakowski BM, Mester Z. 2007. Review of applications of high-field asymmetric waveform ion
1554 mobility spectrometry (faims) and differential mobility spectrometry (dms). Analyst 132:842-
1555 864.
- 1556 Krylov EV. 1999. A method of reducing diffusion losses in a drift spectrometer. Tech Phys+. 44:113-
1557 116
- 1558 Krylov E, Nazarov EG, Miller RA, Tadjikov B, Eiceman GA. 2002. Field Dependence of Mobilities for
1559 Gas-Phase-Protonated Monomers and Proton-Bound Dimers of Ketones by Planar Field
1560 Asymmetric Waveform Ion Mobility Spectrometer (PFAIMS). J. Phys. Chem. A. 106:5437-
1561 5444
- 1562 Krylov EV. 2003. Comparison of the planar and coaxial field asymmetrical waveform ion mobility
1563 spectrometer (FAIMS). Int. J. Mass Spectrom. 225:39-51
- 1564 Krylov EV, Nazarov EG. 2009. Electric field dependence of the ion mobility. Int. J. Mass Spectrom.
1565 285:149-156
- 1566 Kurulugama RT, Nachtigall FM, Lee S, Valentine SJ, Clemmer DE. 2009. Overtone mobility
1567 spectrometry: part 1. experimental observations. J Am Soc Mass Spectrom 20:729-737.
- 1568 Kwasnik M, Fernández FM. 2010. Theoretical and experimental study of the achievable separation
1569 power in resistive-glass atmospheric pressure ion mobility spectrometry. Rapid Commun Mas
1570 Spectrom 24:1911-1918.
- 1571 Langevin P. 1905. Une formule fondamentale de théorie cinétique. Ann Chim Phys 5:245.
- 1572 Lawrence AH. 1986. Ion mobility spectrometry/mass spectrometry of some prescription and illicit
1573 drugs. Anal Chem 58:1269-1272.
- 1574 Levin DS, Vouros P, Miller RA, Nazarov EG, Morris JC. 2004. Characterization of Gas-Phase
1575 Molecular Interactions on Differential Mobility Ion Behavior Utilizing an Electrospray
1576 Ionization-Differential Mobility-Mass Spectrometer System. Anal. Chem.78: 96-106
- 1577 Levin DS, Vouros P, Miller RA, Nazarov EG. 2007. Using a nanoelectrospray-differential mobility
1578 spectrometer-mass spectrometer system for the analysis of oligosaccharides with solvent
1579 selected control over esi aggregate ion formation. J Am Soc Mass Spectrom 18:502-511
- 1580 Li X, Stoll DR, Carr PW. 2009. Equation for peak capacity estimation in two-dimensional liquid
1581 chromatography. Anal Chem 81:845-850.
- 1582 Likar MD, Cheng G, Mahajan N, Zhang Z. 2011. Rapid identification and absence of drug tests for ag-
1583 013736 in 1 mg axitinib tablets by ion mobility spectrometry and dart(tm) mass spectrometry.
1584 J Pharm Biomed Anal 55:569-573.
- 1585 Lipinski CA, Lombardo F, Dominy BW, Feeney PJ. 1997. Experimental and computational
1586 approaches to estimate solubility and permeability in drug discovery and development
1587 settings. Adv Drug Del Rev 23:3-25.
- 1588 Liu H, Yao X, Liu M, Hu Z, Fan B. 2007a. Prediction of gas-phase reduced ion mobility constants ($k(0)$)
1589 based on the multiple linear regression and projection pursuit regression. Talanta 71:258-263.
- 1590 Liu X, Valentine SJ, Plasencia MD, Trimpin S, Naylor S, Clemmer DE. 2007b. Mapping the human
1591 plasma proteome by scx-ic-ims-ms. J Am Soc Mass Spectrom 18:1249-1264.
- 1592 Maitra U, Bag BG, Rao P, Powell D. 1995. Asymmetric synthesis of steroidal Troger's base analogues.
1593 X-ray molecular structure of methyl 3 α ,12 α -{6H,12H-5,11-methanodibenzo[b,f][1,5]diazocine-
1594 2,8-bisacetoxy}-5 β -cholan-24-oate. J. Chem. Soc. Perkin Trans. 1:2049
- 1595 Manard MJ, Trainham R, Weeks S, Coy SL, Krylov EV, Nazarov EG. 2010. Differential mobility
1596 spectrometry/mass spectrometry: The design of a new mass spectrometer for real-time
1597 chemical analysis in the field. Int J Mass Spectrom 295: 138-144
- 1598 Mao Y, Ratner MA, Jarrold MF. 2001. Molecular dynamics simulations of the rehydration of folded
1599 and unfolded cytochrome c ions in the vapor phase. J Am Chem Soc 123:6503-6507.

1600 Martínez-Lozano P, Rus J. 2010. Separation of Isomers L-Alanine and Sarcosine in Urine by
1601 Electro spray Ionization and Tandem Differential Mobility Analysis-Mass Spectrometry. *J Am*
1602 *Soc Mass Spectrom.* 21(7): 1129-1132

1603 Martínez-Lozano P, Criado E, Vidal G, Cristoni S, Franzoso F, Piatti M, Brambilla P. 2011. Differential
1604 mobility analysis-mass spectrometry coupled to XCMS algorithm as a novel analytical
1605 platform for metabolic profiling. *Metabolomics.* 1-14

1606 Mason EA, McDaniel EW, 1988. *Transport Properties of Ions in Gases*, New York: John Wiley & Sons,
1607 560p

1608 Matz LM, Hill HH. 2002a. Evaluating the separation of amphetamines by electrospray ionization ion
1609 mobility spectrometry/ms and charge competition within the ESI process. *Anal Chem* 74:420-
1610 427.

1611 Matz LM, Hill HH, Beegle LW, Kanik I. 2002b. Investigation of drift gas selectivity in high resolution ion
1612 mobility spectrometry with mass spectrometry detection. *J Am Soc Mass Spectrom* 13:300-
1613 307.

1614 McAfee KB, Edelson D. 1963. Identification and mobility of ions in a Townsend discharge by time-
1615 resolved mass spectrometry. *Proc Phys Soc* 81:382-384.

1616 McDaniel EW, Martin DW. 1960. Drift tube-mass spectrometer for studies of thermal-energy ion-
1617 molecule reactions. Technical Report no. 3.

1618 Mie A, Jörntén-Karlsson M, Axelsson B-O, Ray A, Reimann CT. 2007. Enantiomer separation of
1619 amino acids by complexation with chiral reference compounds and high-field asymmetric
1620 waveform ion mobility spectrometry: preliminary results and possible limitations. *Anal Chem*
1621 79:2850-2858.

1622 Milloy HB, Crompton RW. 1977. Momentum-transfer cross section for electron-helium collisions in the
1623 range 4-12 eV. *Phys Rev A* 15:1847.

1624 Momoh PO, El-Shall MS. 2008. Gas phase hydration of organic ions. *Phys Chem Chem Phys*
1625 10:4827.

1626 Myung S, Lee YJ, Moon MH, Taraszka J, Sowell R, Koeniger S, Hilderbrand AE, Valentine SJ,
1627 Cherbas L, Cherbas P, Kaufmann TC, Miller DF, Mechref Y, Novotny MV, Ewing MA,
1628 Sporleder CR, Clemmer DE. 2003. Development of high-sensitivity ion trap ion mobility
1629 spectrometry time-of-flight techniques: a high-throughput nano-lc-ims-tof separation of
1630 peptides arising from a drosophila protein extract. *Anal Chem* 75:5137-5145.

1631 Nazarov EG, Coy SL, Krylov EV, Miller RA, Eiceman GA. 2006. Pressure Effects in Differential
1632 Mobility Spectrometry. *Anal. Chem.* 78: 7697-7706

1633 O'Donnell RM, Sun X, Harrington P de B. 2008. Pharmaceutical applications of ion mobility
1634 spectrometry. *Trac Trends Anal. Chem.* 27:44-53.

1635 Pace CN, Treviño S, Prabhakaran E, Scholtz JM. 2004. Protein structure, stability and solubility in
1636 water and other solvents. *Philos Trans Royal Soc (London) B Biol Sci* 359:1225-1234;.

1637 Poornima CS, Dean PM. 1995. Hydration in drug design. 1. multiple hydrogen-bonding features of
1638 water molecules in mediating protein-ligand interactions. *J computer-aided mol des* 9:500-512.

1639 Pouilly J-C, Nieuwjaer N, Pierre Schermann J. 2008. Structure and dynamics of molecules of
1640 pharmaceutical interest in gas phase and in aqueous phase. *Phys. Scr* 78:058123.

1641 Prieto M, Yost RA. 2011. Spherical FAIMS: comparison of curved electrode geometries. *Int. J Ion*
1642 *Mobil. Spec.* 14: 61-69

1643 Pringle SD, Giles K, Wildgoose JL, Williams JP, Slade SE, Thalassinos K, Bateman RH, Bowers MT,
1644 Scrivens JH. 2007. An investigation of the mobility separation of some peptide and protein ions using
1645 a new hybrid quadrupole/travelling wave IMS/oa-ToF instrument. *Int. J. Mass Spectrom.* 261:1-12.

1646 Pris AD, Mondello FJ, Wroczynski RJ, Murray AJ, Boudries H, Surman CM, Paxon TL. 2009.
1647 Improved specific biodetection with ion trap mobility spectrometry (itms): a 10-min, multiplexed,
1648 immunomagnetic elisa. *Anal Chem* 81:9948-9954.

1649 Purves RW, Barnett DA, Eills B, Guevremont R. 2000. Investigation of bovine ubiquitin conformers
1650 separated by high-field asymmetric waveform ion mobility spectrometry: cross section
1651 measurements using energy-loss experiments with a triple quadrupole mass spectrometer. *J*
1652 *Am Soc Mass Spectrom.* 11:738-745

1653 Shvartsburg A, Purves RW. 2010., differential ion mobility spectrometry: nonlinear ion transport and
1654 fundamentals of faims, crc press, taylor and francis group, boca raton, fl 33487-2742, usa
1655 (2009) ISBN 978-1-4200-5106-3 hardcover, 322 pp. *J Am Soc Mass Spectrom* 21:R3-R3.

1656 Rand KD, Pringle SD, Murphy JP, Fadgen KE, Brown J, Engen JR. 2009. Gas-phase
1657 hydrogen/deuterium exchange in a traveling wave ion guide for the examination of protein
1658 conformations. *Anal Chem* 81:10019-10028.

- 1659 Révész Á, Schröder D, Rokob TA, Havlík M, Dolenský B. 2011. In - flight epimerization of a
 1660 *bis* - Träger base. *Angew Chem Int Ed* 50:2401-2404.
- 1661 Roentgen W. 1896. Eine neue art von strahlen 4th ed. Würzburg: Stahel'schen K.B. Hof und
 1662 Universitätsbuch und Kunsthandlung.
- 1663 Ruotolo BT, Giles K, Campuzano I, Sandercock AM, Bateman RH, Robinson CV. 2005. Evidence for
 1664 macromolecular protein rings in the absence of bulk water. *Science* 310:1658-1661.
- 1665 Ruotolo BT, Gillig KJ, Stone EG, Russell DH. 2002a. Peak capacity of ion mobility mass spectrometry:
 1666 separation of peptides in helium buffer gas. *J Chromatog B* 782:385-392.
- 1667 Ruotolo BT, Gillig KJ, Stone EG, Russell DH, Fuhrer K, Gonin M, Schultz JA. 2002b. Analysis of
 1668 protein mixtures by matrix-assisted laser desorption ionization-ion mobility-orthogonal-time-of-
 1669 flight mass spectrometry. *Int J Mass Spectrom* 219:253-267.
- 1670 Rus J, Moro D, Sillero JA, Royuela J, Casado A, Estevez-Molinero F, Fernández de la Mora J. 2010.
 1671 IMS-MS studies based on coupling a differential mobility analyzer (DMA) to commercial API-
 1672 MS systems. *Int J Mass Spectrom*. 298:30-40
- 1673 Rutherford E. 1897. The velocity and rate of recombination of the ions of gases exposed to röntgen
 1674 radiation. *Philosophical Magazine* 5: 44:422.
- 1675 Santos LFA, Iglesias AH, Pilau EJ, Gomes AF, Gozzo FC. 2010. Traveling-wave ion mobility mass
 1676 spectrometry analysis of isomeric modified peptides arising from chemical cross-linking. *J Am
 1677 Soc Mass Spectrom* 21:2062-2069.
- 1678 Schneider BB, Covey TR, Coy SL, Krylov EV, Nazarov EG. 2010a. Planar differential mobility
 1679 spectrometer as a pre-filter for atmospheric pressure ionization mass spectrometry. *Int J
 1680 Mass Spectrom*. 298: 45-54
- 1681 Schneider BB, Covey TR, Coy SL, Krylov EV, Nazarov EG. 2010b. Chemical effects in the separation
 1682 process of a differential mobility/mass spectrometer system. *Anal Chem* 82:1867-1880.
- 1683 Schneider BB, Covey TR, Coy SL, Krylov EV, Nazarov EG. 2010c. Control of chemical effects in the
 1684 separation process of a differential mobility mass spectrometer system *Eur J Mass Spectrom*
 1685 16: 57-71
- 1686 Schultz SG, Solomon AK. 1961. Determination of the effective hydrodynamic radii of small molecules
 1687 by viscometry. *J Gen Physiol* 44:1189 -1199.
- 1688 Shelimov KB, Clemmer DE, Hudgins RR, Jarrold MF. 1997. Protein structure *in vacuo*: gas-phase
 1689 conformations of bpti and cytochrome c. *J Am Chem Soc* 119:2240-2248.
- 1690 Shelimov KB, Jarrold MF. 1997. Conformations, unfolding, and refolding of apomyoglobin in vacuum:
 1691 an activation barrier for gas-phase protein folding. *J Am Chem Soc* 119:2987-2994.
- 1692 Shvartsburg AA, Clemmer DE, Smith RD. 2010a. Isotopic effect on ion mobility and separation of
 1693 isotopomers by high-field ion mobility spectrometry. *Anal Chem* 82:8047-8051.
- 1694 Shvartsburg AA, Danielson WF, Smith RD. 2010b. High-resolution differential ion mobility separations
 1695 using helium-rich gases. *Anal Chem* 82:2456-2462.
- 1696 Shvartsburg AA, Jarrold MF. 1996. An exact hard-spheres scattering model for the mobilities of
 1697 polyatomic ions. *Chem Phys Lett* 261:86-91.
- 1698 Shvartsburg AA, Mashkevich SV, Baker ES, Smith RD. 2007. Optimization of algorithms for ion
 1699 mobility calculations. *J Phys Chem A* 111:2002-2010.
- 1700 Shvartsburg AA, Smith RD. 2008. Fundamentals of traveling wave ion mobility spectrometry. *Anal
 1701 Chem* 80:9689-9699.
- 1702 Shvartsburg AA, Smith RD, Wilks A, Koehl A, Ruiz-Alonso D, Boyle B. 2009a. Ultrafast differential ion
 1703 mobility spectrometry at extreme electric fields in multichannel microchips. *Anal Chem*
 1704 81:6489-6495.
- 1705 Shvartsburg AA, Tang K, Smith RD. 2004. Modeling the resolution and sensitivity of faims analyses. *J
 1706 Am Soc Mass Spectrom* 15:1487-1498.
- 1707 Shvartsburg AA, Tang K, Smith RD, Holden M, Rush M, Thompson A, Toutoungi D. 2009b. Ultrafast
 1708 differential ion mobility spectrometry at extreme electric fields coupled to mass spectrometry.
 1709 *Anal Chem* 81:8048-8053.
- 1710 Siems WF, Wu C, Tarver EE, Hill HHJ, Larsen PR, McMinn DG. 1994. Measuring the resolving power
 1711 of ion mobility spectrometers. *Anal Chem* 66:4195-4201.
- 1712 Siu C-K, Guo Y, Saminathan IS, Hopkinson AC, Siu KWM. 2010. Optimization of parameters used in
 1713 algorithms of ion-mobility calculation for conformational analyses. *J Phys Chem B* 114:1204-
 1714 1212.
- 1715 Smith DP, Knapman TW, Campuzano I, Malham RW, Berryman JT, Radford SE, Ashcroft AE. 2009a.
 1716 Deciphering drift time measurements from travelling wave ion mobility spectrometry-mass
 1717 spectrometry studies. *Eur J Mass Spectrom* 15:113-130.

- 1718 Smith RD, Prasad S, Tang K, Manura D, Papanastasiou D. 2009b. Simulation of ion motion in faims
1719 through combined use of simion and modified sds. *Anal. chem.* 81:8749-8757.
- 1720 Snyder AP, Blyth DA, Parsons JA. 1996. Ion mobility spectrometry as an immunoassay detection
1721 technique. *J Microbiol Meth* 27:81-88.
- 1722 Snyder AP, Harden CS, Brittain AH, Kim MG, Arnold NS, Meuzelaar HLC. 1993. Portable hand-held
1723 gas chromatography/ion mobility spectrometry device. *Anal Chem* 65:299-306.
- 1724 Souza Pessôa G de, Pilau EJ, Gozzo FC, Zezzi Arruda MA. 2011. Ion mobility mass spectrometry: an
1725 elegant alternative focusing on speciation studies. *J. Anal At Spectrom* 26:201.
- 1726 Steiner WE, English WA, Hill HH. 2006. Ion-Neutral Potential Models in Atmospheric Pressure Ion
1727 Mobility Time-of-Flight Mass Spectrometry IM(tof)MSJ. *Phys. Chem. A.* 110:1836-1844
- 1728 Stolzenburg M, McMurry P. 2008. Equations Governing Single and Tandem DMA Configurations and
1729 a New Lognormal Approximation to the Transfer Function. *Aerosol Sci. Tech.* 42, 421-
1730 432 Tabrizchi M, Jazan E. 2010. Inverse ion mobility spectrometry. *Anal Chem* 82:746-750.
- 1731 Tang K, Shvartsburg AA, Lee H-N, Prior DC, Buschbach MA, Li F, Tolmachev AV, Anderson GA,
1732 Smith RD. 2005. High-sensitivity ion mobility spectrometry/mass spectrometry using
1733 electrodynamic ion funnel interfaces. *Anal Chem* 77:3330-3339.
- 1734 Tang X, Bruce JE, Hill HH. 2006. Characterizing electrospray ionization using atmospheric pressure
1735 ion mobility spectrometry. *Anal Chem* 78:7751-7760.
- 1736 Taraszka JA, Gao X, Valentine SJ, Sowell RA, Koeniger SL, Miller DF, Kaufman TC, Clemmer DE.
1737 2005. Proteome profiling for assessing diversity: analysis of individual heads of drosophila
1738 melanogaster using lc-ion mobility-ms. *J Proteome Res* 4:1238-1247.
- 1739 Tarver EE. 2004. External second gate, fourier transform ion mobility spectrometry: parametric
1740 optimization for detection of weapons of mass destruction. *Sensors* 4:1-13.
- 1741 Thalassinos K, Grabenauer M, Slade SE, Hilton GR, Bowers MT, Scrivens JH. 2009. Characterization
1742 of phosphorylated peptides using travelling wave-based and drift cell ion mobility mass
1743 spectrometry. *Anal Chem* 81:248-254.
- 1744 Thomson JJ. 1903. Conduction of electricity through gases. *Nature* 69:74-75.
- 1745 Thomson JJ, Rutherford E. 1896. On the passage of electricity through gases exposed to röntgen
1746 rays. *Phil Mag Series* 5 42:392.
- 1747 Tuovinen K, Paakkanen H, Hänninen O. 2000. Detection of pesticides from liquid matrices by ion
1748 mobility spectrometry. *Anal Chim Acta* 404:7-17.
- 1749 Turner RB, Brokenshire JL. 1994. Hand-held ion mobility spectrometers. *Trac Trends Anal Chem*
1750 13:281-286.
- 1751 Ude S, Fernández de la Mora J, Thomson BA. 2004. Charge-Induced Unfolding of Multiply Charged
1752 Polyethylene Glycol Ions. *J. Am. Chem. Soc.* 126: 12184-12190
- 1753 Uetrecht C, Rose RJ, Duijn E van, Lorenzen K, Heck AJR. 2010. Ion mobility mass spectrometry of
1754 proteins and protein assemblies. *Chem Soc Rev* 39:1633-1655.
- 1755 Valentine SJ, Kulchania M, Barnes CAS, Clemmer DE. 2001. Multidimensional separations of
1756 complex peptide mixtures: a combined high-performance liquid chromatography/ion
1757 mobility/time-of-flight mass spectrometry approach. *Int J Mass Spectrom* 212:97-109.
- 1758 Valentine SJ, Stokes ST, Kurulugama RT, Nachtigall FM, Clemmer DE. 2009. Overtone mobility
1759 spectrometry: part 2. theoretical considerations of resolving power. *J Am Soc Mass Spectrom*
1760 20:738-750.
- 1761 Vautz W, Schwarz L, Hariharan C, Schilling M. 2010. Ion characterisation by comparison of ion
1762 mobility spectrometry and mass spectrometry data. *Int J Ion Mobil Spec* 13:121-129.
- 1763 Vonderach M, Ehrler OT, Weis P, Kappes MM. 2011. Combining ion mobility spectrometry, mass
1764 spectrometry, and photoelectron spectroscopy in a high-transmission instrument. *Anal Chem*
1765 83:1108-1115.
- 1766 Wang B, Valentine S, Plasencia M, Raghuraman S, Zhang X. 2010. Artificial neural networks for the
1767 prediction of peptide drift time in ion mobility mass spectrometry. *BMC Bioinfo* 11:182.
- 1768 Wang Y, Nacson S, Pawliszyn J. 2007. The coupling of solid-phase microextraction/surface enhanced
1769 laser desorption/ionization to ion mobility spectrometry for drug analysis. *Anal Chim Acta*
1770 582:50-54.
- 1771 Wessel MD, Jurs PC. 1994. Prediction of reduced ion mobility constants from structural information
1772 using multiple linear regression analysis and computational neural networks. *Anal Chem*
1773 66:2480-2487.
- 1774 Wessel MD, Sutter JM, Jurs PC. 1996. Prediction of reduced ion mobility constants of organic
1775 compounds from molecular structure. *Anal Chem* 68:4237-4243.

1776 Weston DJ, Bateman R, Wilson ID, Wood TR, Creaser CS. 2005. Direct analysis of pharmaceutical
1777 drug formulations using ion mobility spectrometry/quadrupole-time-of-flight mass
1778 spectrometry combined with desorption electrospray ionization. *Anal. Chem* 77:7572-7580.
1779 Weston DJ. 2010. Ambient ionization mass spectrometry: current understanding of mechanistic
1780 theory; analytical performance and application areas. *Analyst* 135:661.
1781 Williams JP, Lough JA, Campuzano I, Richardson K, Sadler PJ. 2009a. Use of ion mobility mass
1782 spectrometry and a collision cross-section algorithm to study an organometallic ruthenium
1783 anticancer complex and its adducts with a dna oligonucleotide. *Rapid Commun Mass*
1784 *Spectrom* 23:3563-3569.
1785 Williams JP, Bugarcic T, Habtemariam A, Giles K, Campuzano I, Rodger PM, Sadler PJ. 2009b.
1786 Isomer separation and gas-phase configurations of organoruthenium anticancer complexes:
1787 ion mobility mass spectrometry and modeling. *J Am Soc Mass Spectrom* 20:1119-1122.
1788 Williams JP, Grabenauer M, Holland RJ, Carpenter CJ, Wormald MR, Giles K, Harvey DJ, Bateman
1789 RH, Scrivens JH, Bowers MT. 2010. Characterization of simple isomeric oligosaccharides and
1790 the rapid separation of glycan mixtures by ion mobility mass spectrometry. *Int J Mass*
1791 *Spectrom* 298:119-127.
1792 Wren SAC. 2005. Peak capacity in gradient ultra performance liquid chromatography (uplc). *J Pharm*
1793 *Biomed Anal* 38:337-343.
1794 Wright P, Alex A, Nyaruwata T, Parsons T, Pullen FS. (2010). Using density functional theory to
1795 rationalise the mass spectral fragmentation of maraviroc and its metabolites. *Rapid Commun*
1796 *in Mass Spectrom*, 24: 1025–1031
1797 Wu C, Siems WF, Asbury GR, Hill HH. 1998. Electrospray ionization high-resolution ion mobility
1798 spectrometry–mass spectrometry. *Anal Chem* 70:4929-4938.
1799 Wyttenbach T, Kemper PR, Bowers MT. 2001. Design of a new electrospray ion mobility mass
1800 spectrometer. *Int J Mass Spectrom* 212:13-23.
1801 Wyttenbach T, Paizs B, Barran P, Brechi L, Liu D, Suhai S, Wysocki VH, Bowers MT. 2003. The effect
1802 of the initial water of hydration on the energetics, structures, and h/d exchange mechanism of
1803 a family of pentapeptides: an experimental and theoretical study. *J Am Chem Soc*
1804 125:13768-13775.
1805 Zhao W, Bhushan A, Schivo M, Kenyon NJ, Davis CE. 2010. Miniature differential mobility
1806 spectrometry (dms) advances towards portable autonomous health diagnostic systems. In:
1807 *Wearable and autonomous biomedical devices and systems for smart environment*. Springer
1808 Berlin Heidelberg. Lecture Notes in Electrical Engineering Vol. 75, p. 55-73.
1809 http://dx.doi.org/10.1007/978-3-642-15687-8_3.
1810 Zhou M, Robinson CV. 2010. When proteomics meets structural biology. *Trends Biochem Sci* 35:522-
1811 529.
1812 Zhu M, Bendiak B, Clowers B, Hill HH. 2009. Ion mobility-mass spectrometry analysis of isomeric
1813 carbohydrate precursor ions. *Anal Bioanal Chem* 394:1853-1867.
1814 Zolotov YA. 2006. Ion mobility spectrometry. *J Anal Chem* 61:519-519.
1815
1816